Instituto Superior
de Engenharia
Politécnico de Coimbra

DEPARTAMENTO DE / DEPARTMENT OF
MECHANICAL ENGINEERING

Development of a Fixing and Adjusting Device for Chevron Osteotomy

Project Report to fulfill the Master's degree in Mechanical Engineering

Specialization in Construction and Maintenance of Mechanical Equipments

Author

Mariana Costa Santos

Supervisor

Luis Manuel Ferreira Roseiro

INSTITUTO POLITÉCNICO
DE COIMBRA

INSTITUTO SUPERIOR
DE ENGENHARIA
DE COIMBRA

Coimbra, July 2023

RESUMO

O Hallux Valgus é uma deformação que ocorre no primeiro metatarso do pé, podendo em alguns casos atingir também a falange. O tratamento desta deformação obriga, na maioria das situações, a um procedimento cirúrgico. A Osteotomia de Chevron é o tipo de cirurgia habitualmente implementada, sendo os cortes e perfuração do osso normalmente realizados pelo cirurgião sem o recurso a dispositivos específicos de apoio e guiamento. A possibilidade de desenvolver um dispositivo de apoio que permita aumentar a precisão na realização desta cirurgia foi o foco deste trabalho de Mestrado. Este trabalho apresenta um novo dispositivo para apoio na execução da Osteotomia de Chevron, desenvolvido em estreita colaboração com uma equipa de Ortopedistas. Inicialmente foi feita uma identificação da técnica e dos procedimentos associados à cirurgia de Chevron. Depois foi desenvolvido um modelo 3D de um metatarso, que serviu de base ao desenvolvimento do conceito do dispositivo. O dispositivo desenvolvido incorpora diferentes configurações, tendo como base uma estrutura puramente mecânica.

O Protótipo do dispositivo foi produzido com tecnologias de fabrico aditivo e com recurso a materiais e componentes compatíveis com a sua utilização em contexto real. A evolução na conceção do dispositivo mostrou a identificação de características que permitiram o seu teste experimental com a aquisição de dados associados à precisão de corte. Os resultados evidenciaram adequada robustez do dispositivo, que pode desempenhar uma missão de relevo no apoio ao processo cirúrgico da osteotomia de Chevron.

Palavras-chave: Pé, Hallux Valgus, Osteotomia de Chevron, Biomecânica ortopédica

ABSTRACT

Hallux Valgus is a deformation that occurs in the foot's first metatarsal, and in some cases, it can also reach the phalanx. The treatment of this deformation requires, in most situations, a surgical procedure. Chevron Osteotomy is the type of surgery usually implemented, with the cuts and drilling of the bone normally performed by the surgeon without specific support and guidance devices. The possibility of developing a support device that allows to increase the precision in performing this surgery was the focus of this Master's Thesis. This work presents a new device to support the execution of the Chevron Osteotomy, developed in close collaboration with a team of Orthopedists. Initially, an identification of the technique and procedures associated with the Chevron surgery was carried out. Afterwards, a 3D model of a metatarsal was developed, which served as the basis for the development of the device concept. The developed device incorporates different configurations, based on a purely mechanical structure.

The prototype of the device was produced using additive manufacturing technologies and materials and components compatible with its use in a real context. The evolution in the device's design showed the identification of characteristics that allowed its experimental test with the acquisition of data associated with cutting precision. The results showed adequate robustness of the device, which can play an important role in supporting the surgical process of Chevron osteotomy.

Keywords: Foot, Hallux Valgus, Chevron Osteotomy, Orthopedic Biomechanics

DEDICATION

Dedico este trabalho aos meus pais.

THANKS

To my parents, Maria Lucia, and Rui, who gave me values and motivation to be able to fight for my goals.

To Professor Dr. Luis Roseiro, who, in addition to being my advisor and the key that opened the door to biomechanics, was a source of knowledge and wisdom that supported me and believed in me to overcome the challenges that were proposed to me throughout work. I also thank you for all your companionship and presence as a friend throughout the work, both inside and outside.

To Mr. Dr. Emanuel Seiça for making available his limited time tirelessly and his availability to share his wisdom that enriched this work. I also thank you for allowing me to build and develop something that will improve a surgical process, leaving my mark in orthopedics.

To Professor Vitor Maranha for his vision, words of encouragement, and motivation that helped to feel capable of carrying out this project.

To Rafael Carvalho, for all the support and encouragement given throughout this work.

To my colleagues and friends Inês Cruz and Luís Pardal, for sharing the moments when, many times, the strength to continue seemed to want to disappear but the good mood that reigned in that laboratory solved the situation. I also appreciate all the sharing of ideas that allowed the evolution of this work.

To my friends, for all the support given throughout this work.

To all of you, once again, my thanks and most sincere recognition for your contribution.

INDEX

INDEX OF FIGURES

LIST OF ABBREVIATIONS AND ACRONYMS

AISI	American Iron and Steel Institute
CAD	Computer Aided Design
CT	Computed Tomography
DIJ	Distal Interphalangeal Joint
FDA	Food and Drug Administration
FFF	Fused Filament Fabrication
HVA	Hallux Valgus
IMA	Intermetatarsal Angle
LBA	Laboratory of Applied Biomechanics
MT	Metatarsus
MTP	Metatarsophalange
PET	Polyethylene terephthalate
PIJ	Proximal Interphalangeal Joint
PU	Polyurethane
RIHUC	Institutional Repository of Hospitals of the University of Coimbra
STL	Standard Triangle Language
TPU	Thermoplastic polyurethane
3D	Three dimensions

LIST OF SYMBOLS

Latin Alphabet

C	Adjustment on the rail in the long arc
L_C	Longitudinal adjustment of the cutting adjustment system
L_D	Longitudinal adjustment of the drilling system
L_F	Longitudinal adjustment of the fixation system
x	x axis of rotation
y	y axis of rotation

Greek Alphabet

α	Adjusting the angles between the two long bars of the cutting adjustment system
β	Adjustment of the radial variation of the cutting adjustment system
γ	Adjusting the angle around x axis
ψ	Adjusting of the angle around y axis
φ	Rotational adjustment of the fixation system
ρ	Drilling system rotational adjustment

1 INTRODUCTION

This chapter presents a contextualization of the work, objectives and methodology followed, as well as the organization of the writing of this document.

1.1 Framework

Hallux Valgus (HVA) is a pathology commonly known as a bunion. This presents a deviation of the big toe towards the remaining toes, forming a bony protrusion. The deviation is designed Valgus. In most cases, an individual with HVA needs to be forward to surgery techniques. There are several procedures to perform the HAV surgery, being the Chevron Osteotomy one of the most used (Martins, 2013). The Chevron Osteotomy consists of cutting the first metatarsal of the affected foot and positioning it to eliminate the discomfort or pain associated with the pathology and the visual appearance. Despite its wide applicability, the adherence to implement the Chevron Osteotomy is not total, mainly due to the risk of recurrence, due to the lack of guidance from the surgeon to perform the cutting procedures.

Currently, according to the author's knowledge, the market doesn't offer aids to support this process, and the procedure is mainly manual being done according to the surgeon's experience. Only one device with several limitations can be found in literature to support the technique associated with Chevron Osteotomy (Patent No. CN211381609U, 2020). This device presents several limitations and is not available on the market.

In this sense, the development of a device that allows the improvement of the implementation of the Chevron technique would be an important step in the advancement of science and technique associated with the correction of HVA. The possibility of being an integral part and designer of such a device and contributing to these advances represents a motivating factor for the author.

The project involved reverse engineering methodologies, Three Dimensions (3D) modeling, and additive manufacturing techniques.

The evolution in the device's conception showed the identification of characteristics that allowed its experimental test.

The results demonstrate adequate resistance and stability and its usability, evidencing that the device can play an essential role in supporting the Chevron osteotomy.

1.2 Objectives and Methodology

The author of the work, who was the principal member of a team that included an orthopedist, carried out the project for the new device. The main objective of this work involved the design of a new biomechanical device for stabilizing and guiding of Chevron Osteotomy surgical procedures, mainly the cutting and drilling steps. The final objective with the device is to help making the process more reliable, stable, and with less possibility of reappearance due to lack of guidance. Then, the main objective is to develop a functional mechanical device.

The development of the device was established through the definition of an execution schedule whose steps begin with developing a concept of use and a 3D CAD (Computer Aided Design) model of a general geometry to support it. The 3D models were implemented using Solidworks® software.

The device concept leads to a first prototype that undergoes with a compromise between geometry, functionality, production, and simplicity of use. This link was obtained on two relevant levels: a) Clinical compliance, emphasizing the execution of the Chevron osteotomy technique; Ease of production through additive manufacturing, with a design that simplifies the 3D printing process.

To support the development of the device, a 3D model of a metatarsus bone was also implemented. The bone model was obtained from a Computed Tomography (CT) scan, with the help of Slicer 3D® and Geomagic® software, and produced with a mix methodology, based on additive manufacturing for the cortical region, followed by the injection of material to fill out the trabecular region.

Considering the device prototype and the bone model, some experimental tests were implemented, based on the implementation of the Chevron Osteotomy. Additive manufacturing was implemented, with the integral production of the structural elements of the device from Fused Filament Fabrication (FFF) technology. The first experimental tests have been done by an Orthopedist.

1.3 Work Structure

The writing of this work involves the description of the steps taken until obtaining the final geometry of the prototype of the device developed and its first experimental tests. The work is organized into 6 chapters:

Chapter 1 – Introduction

This chapter is dedicated to defining the motivation, objectives, and methodology of the work;

Chapter 2 – Literature Review

This chapter describes the bibliographic review that was carried out, considered fundamental for this work. The research covers the original disease, the associated

pathologies, anatomy, biomechanics, and the state of the art in relation to existing devices for aiding in the surgery of Hallux Valgus (HVA) pathology;

Chapter 3 – Bone Model Development

This chapter explains the methodology used to develop and obtain a 3D and real model of a metatarsus bone, relevant for the device development;

Chapter 4 – Support Device Development

The chapter 4 expose the final prototype and all the methodology used to obtain the device's concept, the 3D model, and its production;

Chapter 5 – Device Experimental Evaluation

The developed device was experimentally tested in a laboratory context. This chapter shows the protocol considered, tests performed, and results obtained as its discussion;

Chapter 6 – Conclusions and Future Developments

The chapter 6 explains the main conclusions of this work, as well as the future developments to be carried out to improve it;

The bibliographical references used to support the project development can be consulted after the chapter 6. Finally, at the end of the document, several Appendix documents are exposed.

2 LITERATURE REVIEW

This chapter describes the literature review that was carried out, considered fundamental for this work. The research covers the original pathology, the associated pathologies, anatomy, biomechanics, and the state of the art in relation to existing devices for aiding in the surgery of Hallux Valgus (HVA) pathology.

2.1 Foot Anatomy

The human foot comprises 26 bones, divided into three main groups: tarsus (tarsal bones (7); metatarsal bones (5), which are part of supporting body weight; phalanges (14). The main human foot bones can be observed and identified in Figure 2.1 (Kenhub, Bones of the foot, 2023).

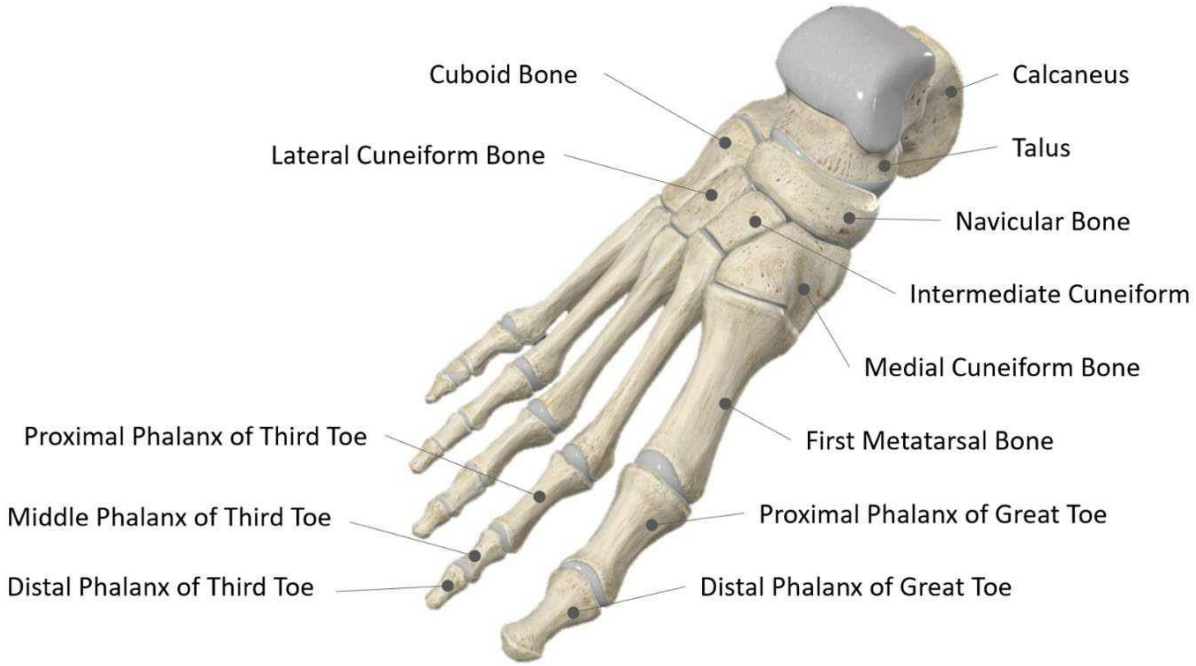

Figure 2.1 - Foot bones, adapted from 3D4Medical, (2016).

The bones are interconnected by several joints, which can be classified into four groups: intertarsal joints, which are between the tarsal bones; tarsometatarsal joints, which are between the tarsal bones and the metatarsal bones; metatarsophalangeal joints, which lie between the heads of the metatarsal bones and the corresponding bases of the proximal phalanges of the foot; interphalangeal joints, which are between the phalanges of the foot. Four of the toes have a proximal interphalangeal joint (PIJ) and a distal interphalangeal joint (DIJ), while the other, the hallux (big toe), has only one interphalangeal joint. In Figure 2.2, it is possible to observe the clarified composition (Kenhub, Joints and ligaments of the foot, 2023).

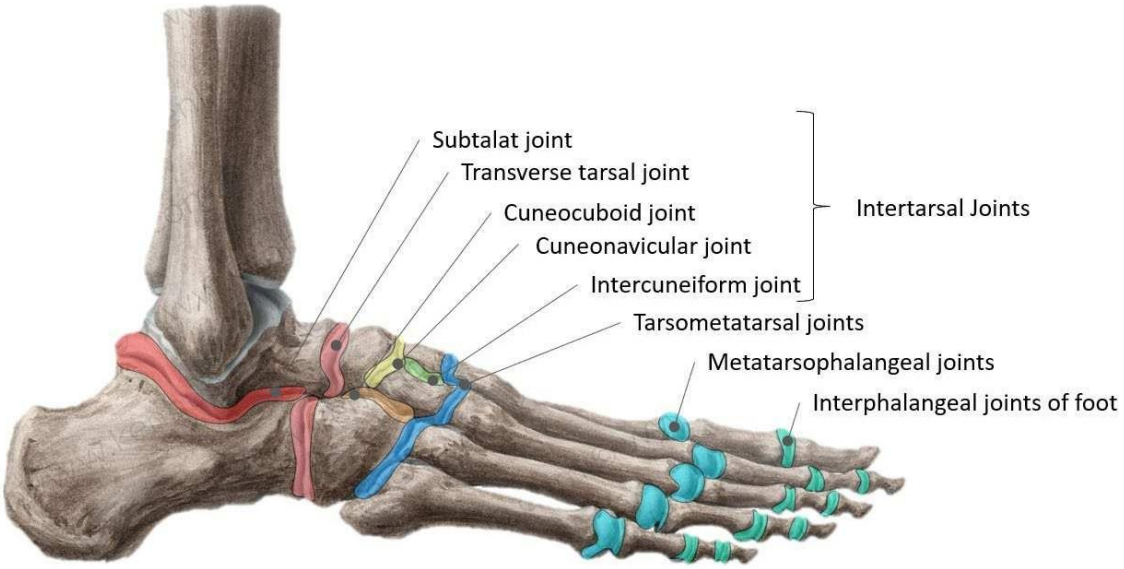

Figure 2.2 - Foot joints, adapted from Ken hub, "Joints and ligaments of the foot", (2022).

Underpinning all the above are the muscles contributing to dorsiflexion, toe movements, and plantar flexion. These are divided into two groups: plantar (which subdivide into lateral, central, and medial) and dorsal (which are just two muscles). The dorsal muscles promote the extension of the fingers, which in turn incorporate the extensor hallux short muscle and the extensor short muscle. The lateral plantar muscles act on the fifth toe, the opposing muscles of the little finger, the flexor muscle short, and the abductor of the little finger. The central plantar muscles act on the four lateral toes, the four dorsal interosseous muscles, the three plantar interosseous muscles, the flexor muscle short and quadratus plantar muscles, and the four lumbrical muscles of the foot (Kenhub, Muscles of the foot, 2023). The medial plantar muscles act on the big toe, the hallux, which is the adductor, abductor, and flexor hallux short muscles Figure 2.3.

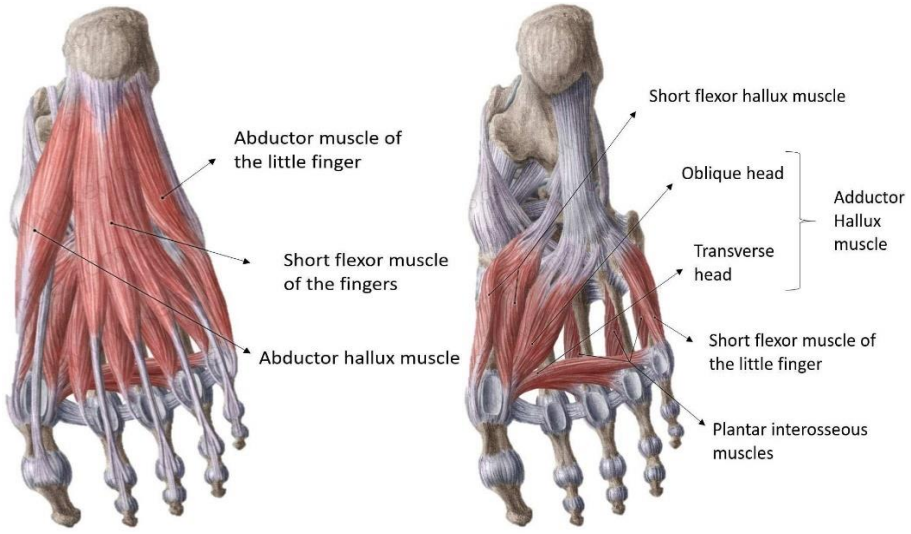

Figure 2.3 - Foot muscles, adapted from Ken hub, "Muscles of the foot", (2022).

2.2 Hallux Valgus (HVA)

The HVA is the most frequent deformation of the metatarsophalangeal joint, which consists of lateralization of the hallux due to a significant deviation of the first metatarsal. According to a systematic review (Nix, Smith, & Vicenzino, 2010), this deformation occurs mainly in adults, with an estimated prevalence of 23% in the 18-65 age group and 35.7% over 65 years. The prevalence is higher in females (30%) than in males (13%), increasing with age. In some feet, there is a genetic predisposition to non-linear bone alignment or laxity of the static stabilizers that disturbs this muscle balance. Inadequate footwear is essential in speeding up the process, but occupancy and excessive walking and weight-bearing are unlikely to be notable factors.

Many inherent or acquired biomechanical abnormalities are identified in HVA feet. However, these associations are incomplete and non-linear.

In any patient, several factors come together to cause HVA. Once this complex pathogenesis unravels, a more scientific approach to managing HVA will be possible, thus allowing the treatment (conservative or surgical) adjustable to the individual (Perera, Mason, & Stephens, 2011). An explanatory scheme is presented in Figure 2.4.

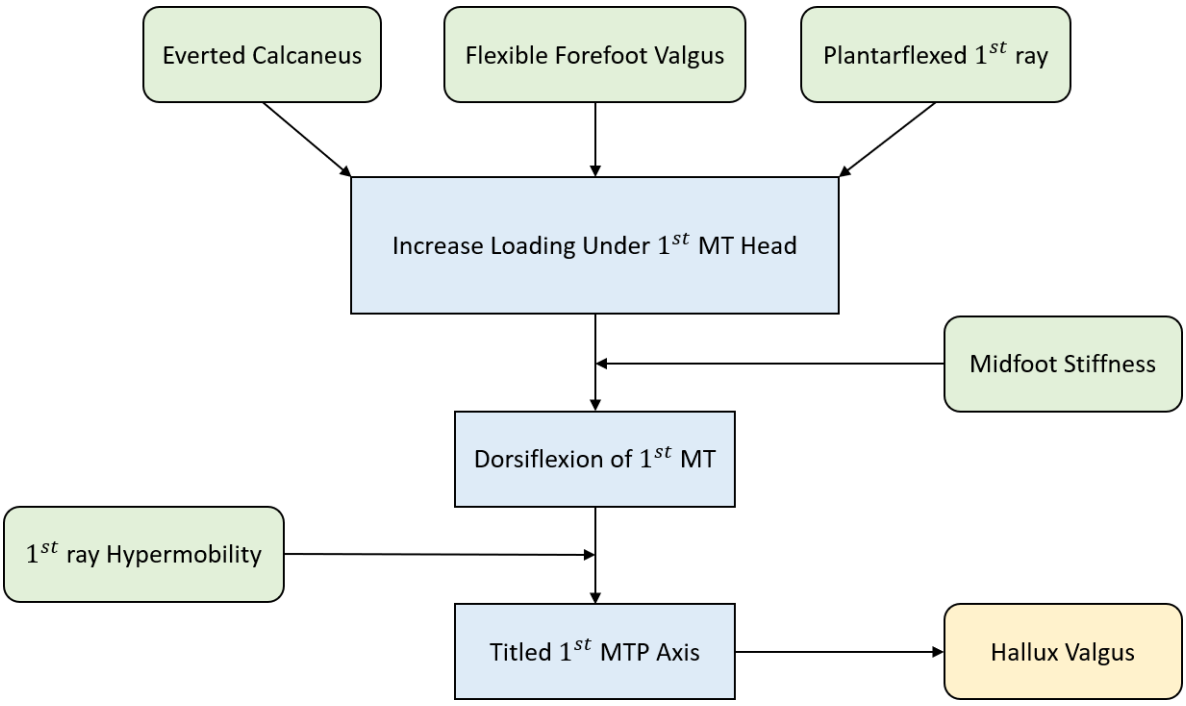

Figure 2.4 - Scheme of the main factors that can lead to HVA, adapted from (Perera, Mason, & Stephens, 2011).

There is an association between the use of tight, high-heeled shoes and deformity, illustrated by the higher incidence among mentioned shoes than non-users, probably due to the chronic pressure exerted on the hallux. However, not all users of tight

shoes develop HVA, suggesting the need for intrinsic factors that ensure feet are more susceptible to the effects of footwear (Sorrisos, 2023).

The resulting imbalance of the first metatarsophalangeal joint contributes to the worsening of the deformity, with subluxation of the articular surface of the proximal phalanx over the head of the first metatarsal. Gradually, the formation of a prominence called a bunion or bunion observe. Lateral capsular tension eventually leads to subluxation and fixation of the sesamoid bones in a lateral position. The deformity accentuates by the lateral slipping of the long extensor and flexor hallux lengthy, which act as adductors. Eventually, pronation of the first finger is observed due to stretching of the dorsomedial region of the joint capsule and rotation of the proximal phalanx by the abductor hallux tendon. The evolution culminates in osteoarthritis of the metatarsophalangeal joint and the degradation of neighboring fingers by compression (Sharma & Aydogan, 2015). We can see the difference between a healthy foot and a foot with hallux valgus in Figure 2.5.

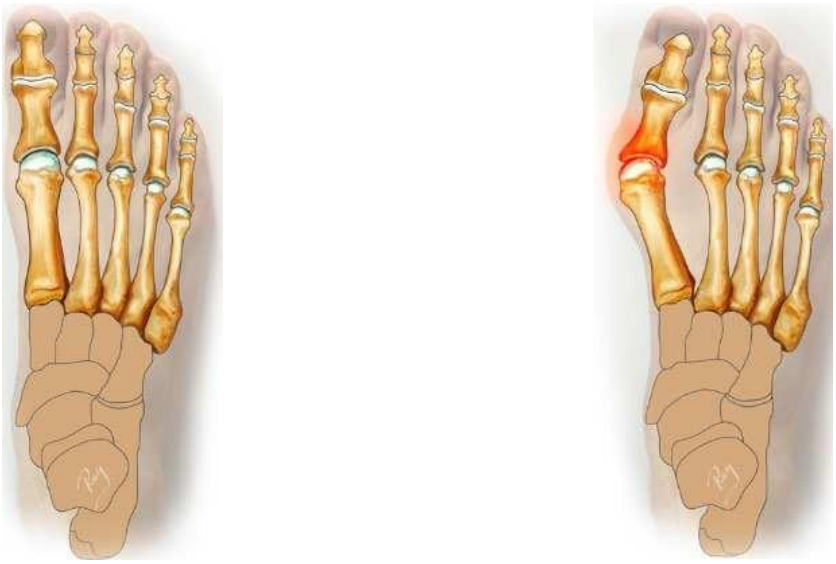

a) b)

Figure 2.5 - Image comparing: a) Normal foot, with relative parallelism between the five metatarsal bones and their respective toe; b) Foot with Hallux Valgus, with bunion - with rotation of the first metatarsal and toe. Adapted from (pied, 2023)

There are Hallux Valgus (HVA) and intermetatarsal (IMA) angles that characterize the deformity as mild, with HVA angles <30º and IMA <13º, moderate, with HVA angles 30-40º and IMA 13-20º, and severe, with HVA >40º and IMA >20º (Cohen, Richardson, & Fernandes, 2010). Radiographic measurement allows this analysis and anticipates the necessary impact of the surgical intervention on hallux realignment and provides essential help in selecting the appropriate procedure or combination of techniques (Nguyen, Sullivan, Alpuerto, Mueller, & Sly, 2019).

2.3 HVA Surgery for Deformity Correction

Corrective treatment of the HVA deformity inevitably involves surgical intervention. More than 100 different surgical procedures are currently described, many of which represent only slight technical variations. The focus here is the Distal Chevron Osteotomy (Figure 2.6), which consists of the side translation of a distal fragment that contains the head of the first metatarsal, produced by the transition in the sagittal plane of an angle of 60º from the distal apex. The resulting medial exostosis is excised, with subsequent plication of the medial capsule (Lerat, 2011) (Jahss, 1991) (Bascarević, et al., 2011).

Figure 2.6 - Distal Chevron osteotomy. From, Martins, P. P., (2013).

This procedure involves several steps. The first is to make the incision, which is carried out according to clinical and fluoroscopic markings to allow visualization of the site to be treated and the release of soft tissues. Afterwards, two Kirschner wires are fixed in the first metatarsal. In a second phase, the Chevron osteotomy is performed, with a saw equipped with a cutting blade, initially positioning this in the neck of the first metatarsal, intending to obtain a "V"-shaped osteotomy with a perpendicular angulation to the medial cortex, performing first the dorsal cut and then the plantar cut. In the third phase, the distal fragment is moved as much as possible to the lateral region, and the osteotomy is fixed percutaneously with two cannulated headless screws. Finally, the surgical area is cleaned with saline, and the incisions are sutured.

According to the research implemented, only one device had been found published, aiming to assist in HVA surgeries, Zixuan L. et al., 2022. The invention (Figure 2.7) allows guiding the cut using fixed guides. However, it is a device with several limitations, being a static device, with three fixed fixation positions, and without the possibility of angular adjustment.

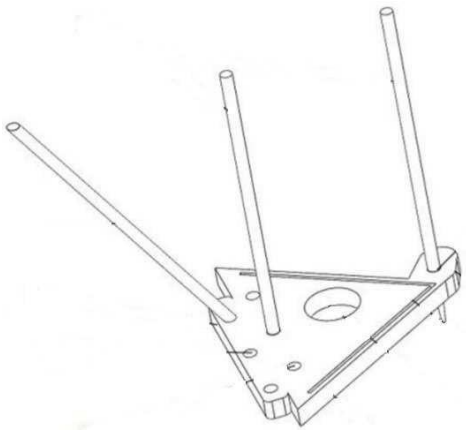

Figure 2.7 - Invention (Patent No. CN211381609U, 2020).

Given the literature review, as the experience of the medical team from the project, there is a lack of devices to help the performance of HVA surgery, particularly to guide the blade and drill with a predefinition and adjustment of the cut and drill position. This opens the door of improvement and innovation and motivates the research to project a device that can allow and guarantee greater precision in the cutting and bone fixation during the Chevron Osteotomy.

3 BONE MODEL DEVELOPMENT

The development of the device initially involved a thorough analysis of the entire cutting procedure associated with the Chevron osteotomy. In this step, specific criteria for blade positioning and necessary adjustments were established to ensure optimal alignment and stabilization of the cutting blade. So that this analysis could be done, it was necessary to have a bone reference, particularly the metatarsus. This chapter describes the procedures follow to obtain the 3D geometry of the toes.

The team of the project decided to use a healthy foot as a reference, considered indicated to obtain a reference 3D model of the foot bones. The 3D geometry of the toes, including the first metatarsal and the phalanx, was obtained from a computed tomography (CT) of a human foot.

3.1 From CT scan to STL (Standard Triangle Language) Model

The Slicer 3D® software is an open-source software that can be used for visualization and segmentation of 3D images, particularly medical files. The focus of this software is on biomedical applications. In this project, the Slicer 3D® software was used, where segmentation techniques were applied and the use of image filters to accurately delineate the bone and its trabecular and cortical regions. It is possible to carry out this process in an iterative way, slice by slice, pre-selecting the area of interest, or in a semi-automatic way, using the thresholding tool, which allows a demarcation according to the defined range to be able to pre-select the areas. The Figure 3.1 shows the layout of the Slicer 3D® software with the foot file imported and the corresponding.

Figure 3.1 - Visualization of using the Threshold tool in CT, in Slicer 3D®.

After the initial step and the definition of the segmentation filters, it is possible to obtain a render model, helping the visualization of the foot. The model can be optimized and cleaned according to the project objectives, using the software tools to erase. In this case, it was only intended to have the model of the first metatarsal and phalanx. Then, the model was cleaned slice by slice and as can be seen in Figure 3.2, the model with only the first metatarsal and the phalanx was obtained.

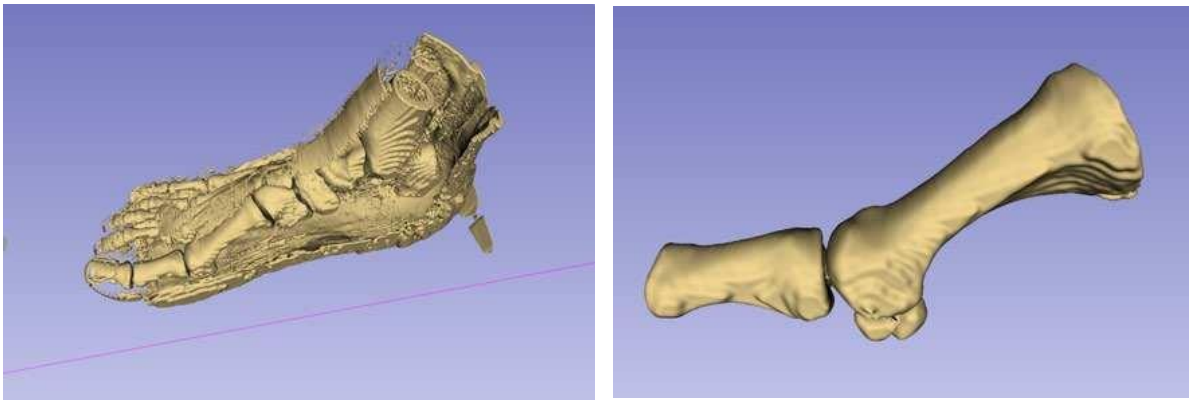

a) b)

Figure 3.2 - CT rendering, in Slicer 3D®: a) Initial model; b) Model sectioned with only the first metatarsal and phalanx.

After this step, it was important to select and separate the cortical and trabecular bone. This was made by selecting the areas to be obtained in the STL (Standard Triangle Language), as can be seen in Figure 3.3.

a) b)

Figure 3.3 - CT visualization with selection of the region to be segmented: a) CT top view; b) Lateral CT view.

Using the software tools "grow" the regions corresponding to cortical and trabecular bone were separated. In this case, it was decided to select the cortical and the

trabecular zones to have a better precession of the delimitations, as shown in Figure 3.4.

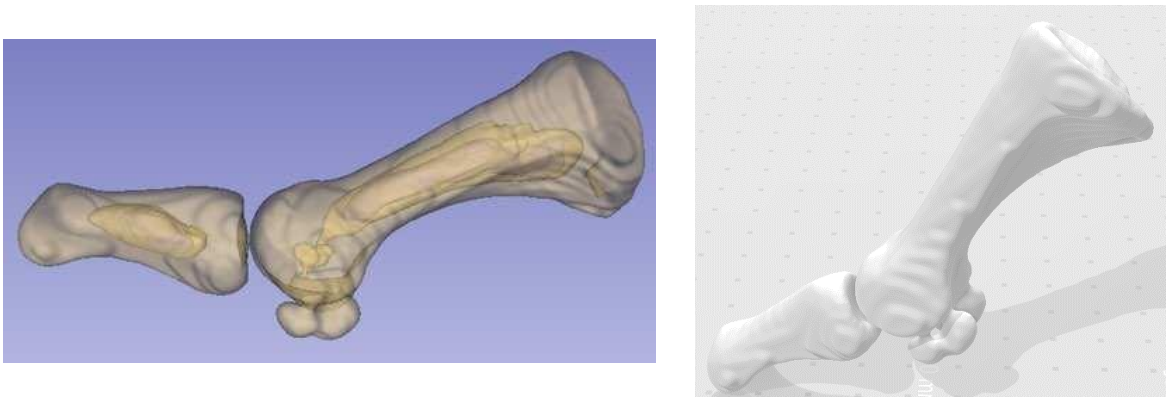

a) b)

Figure 3.4 - Visualization: a) Model of the first metatarsal and phalanx, separating the cortical and trabecular regions; b) STL Model.

3.2 From STL to 3D Model

Using the smoothing tools from the software, the model was standardized so that the STL to be created does not have protrusions, being as organic as possible to allow the following procedures. This STL transformation and optimization is represented in Figure 3.5.

a) b)

Figure 3.5 - STL optimization: a) Complete model; b) Sectioned model.

The last step to obtain the 3D geometry of the bones evolves the transforming of STL file into a solid body. The procedure was implemented thought the Geomagic® Software, a reverse engineering tool. The Geomagic® considered in this project run as an add-in toll inside the 3D modeling software Solidworks®. Then, each software was used in this step.

The Geomagic® software allows the optimization of the triangulation of geometry, excluding loose points, disproportionate zones, and flaws in the model so that it is

possible to create an organic 3D model from the STL, allowing its manipulation, as intended. The model was treated to be functional for the intended design of the device, as also to be an important part in the experimental tests, as explained later in Chapter 5, opting only for the use of the metatarsus, as can be seen in Figure 12b).

After this transformation, it was decided to optimize the definition of the trabecular regions. As the CT conversion presents some reading errors found in the analysis of this bone component, opting to measure the maximum height of the trabecular zone read by the thickness of the program and standardize it along the total length of the metatarsus. In Figure 3.6, the final 3D model can be seen, with great separation of the cortical and trabecular zones.

The global dimensions of a metatarsal considered medium are 66 (mm) in length and an average height of 23 (mm), these dimensions are based on the CT metatarsal. These dimensional references were considered in the development of the device.

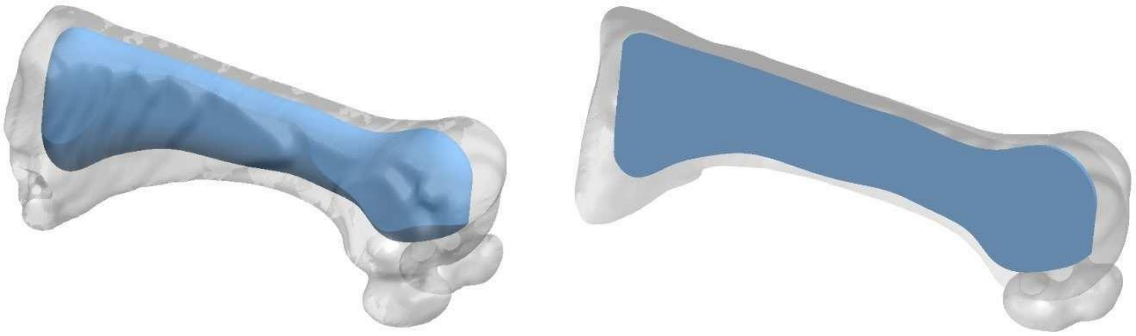

a) b)

Figure 3.6 - Visualization of the 3D model of the metatarsal: a) Complete model; b) Sectional model.

4 SUPPORT DEVICE DEVELOPMENT

The development of the device proposed in this work, designated as Fixing and Adjusting Device for Chevron Osteotomy, followed the alignment shown in the diagram in Figure 4.1. The main stages of device development are the idealization of the geometry, in parallel with the idealization of the operation principle. The next step involves the development of the 3D virtual model and producing the prototype, ending the cycle with the production/validation of the final prototype.

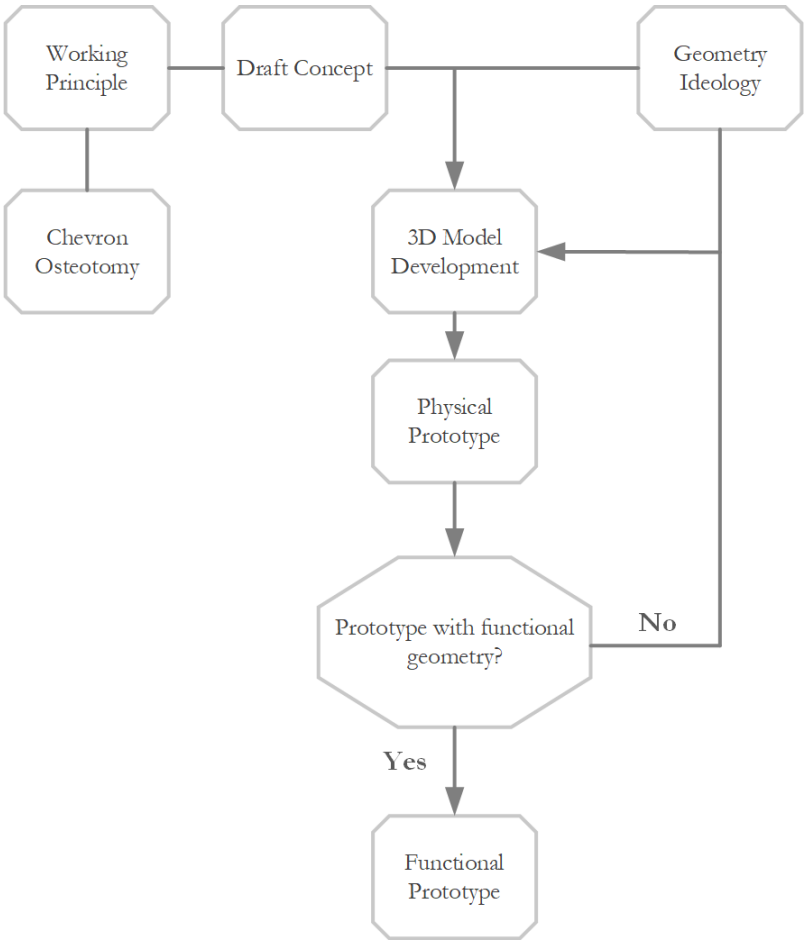

Figure 4.1 - Device development flow diagram.

4.1 Device Prototype

The concept of the developed device is present in the Figure 4.2, which shows the first draft. Knowing that the Chevron procedure starts with two Kirschner wires, the idea of the prototype is based on a circular device with two rings, to be clamped to the wires. Inside the rings a set of 3 adjusted bars acts as a guide for the cutting blade.

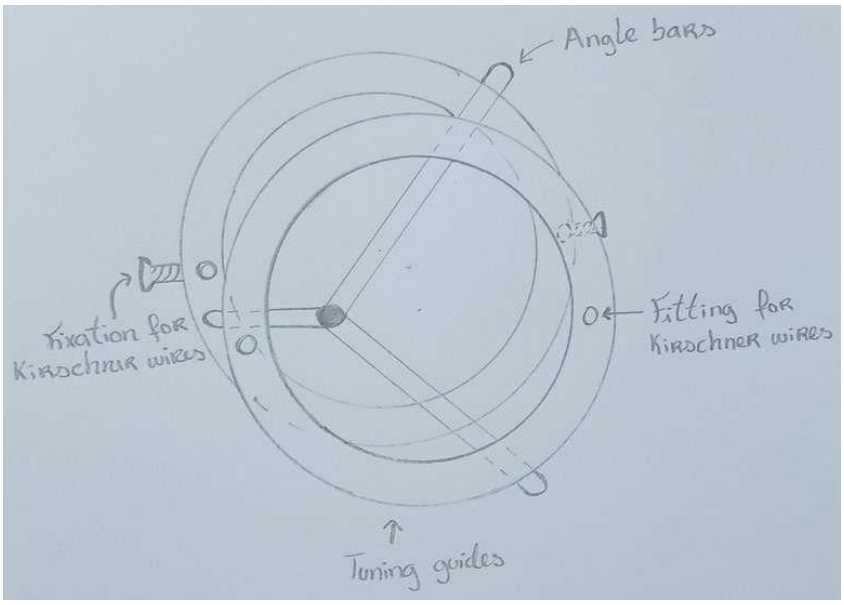

Figure 4.2 - First draft of the device concept.

The development of the device involved several versions from the first draft. The author's option was to present the final model explaining its concept. The Figure 4.3 shows the final model of the device prototype, coupled in a metatarsal bone model. The device's operating mechanism is designed to obtain detailed and accurate regulation and adjustment. Considering the acquired dimensions of the metatarsal model, the device was developed according to the Chevron surgery procedure and the surgical conditions.

The global dimensions of the device with assembly components reach 82 (mm) height and 58 (mm) width.

Figure 4.3 - 3D render visualization of the final model of the device prototype.

4.1.1 Device Prototype Components and Assembly

The device can be divided into four main sub-systems (Figure 4.4), namely: 1. Fixation system; 2. Cutting regulation system; 3. Angular adjustment system; 4. Drilling guidance system. All the mechanical components and geometric details and dimensions can be found in the Appendix A. The description of each system is now exposed.

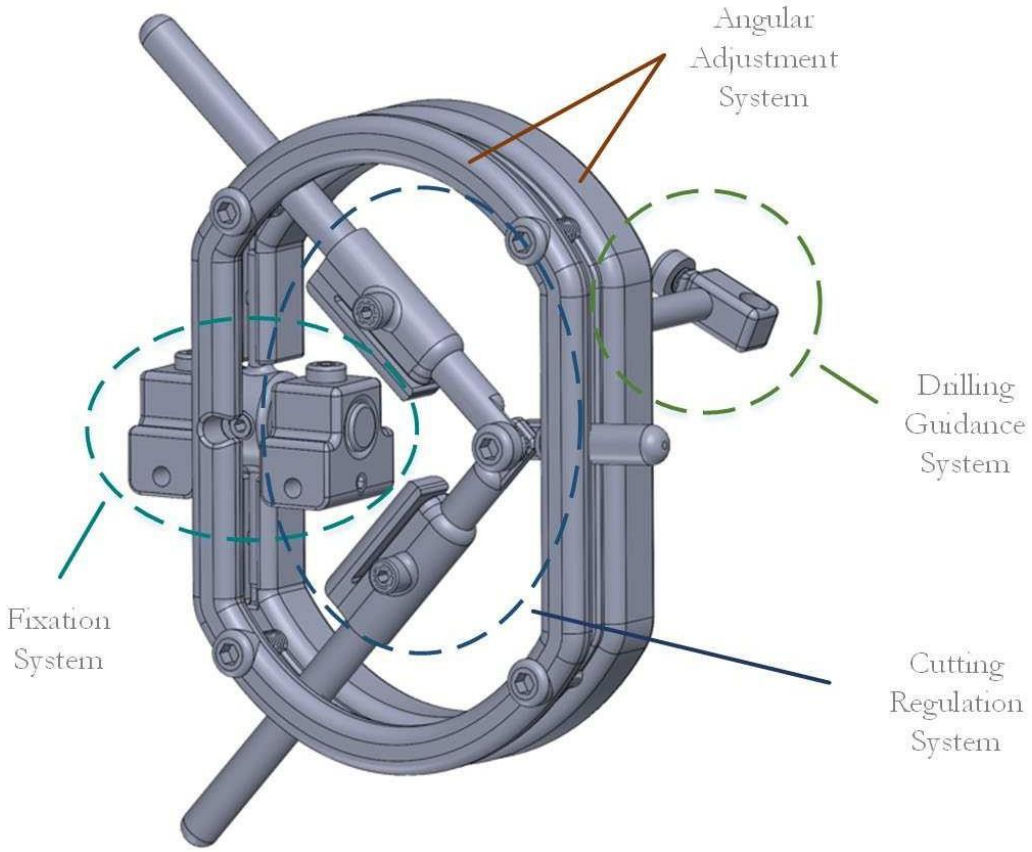

Figure 4.4 - Representation of the various device systems.

Fixation System

As exposed, the idea was to have an anchorage of the system in the two Kirshner wires, normally used in the Chevron technique. To provide this, a fixation system was designed and are represented in Figures 4.5 and 4.6. The system consists of main blocks where the Kirschner wires are inserted. The blocks are fixed together by a central bar with two screws.

The system is fixed to the Kirschner wires with two screws allowing the longitudinal adjustment of the fixation system (L_F). In the central part of the bar, an angular pendulum element allows the fixation of the angular system and the definition of its position (φ).

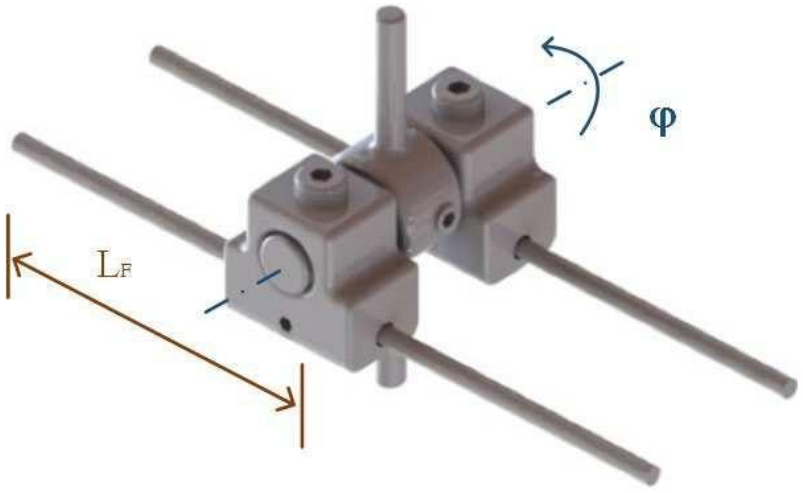

Figure 4.5 - Representation of rendered model of the fixation system with the longitudinal and rotational adjustments.

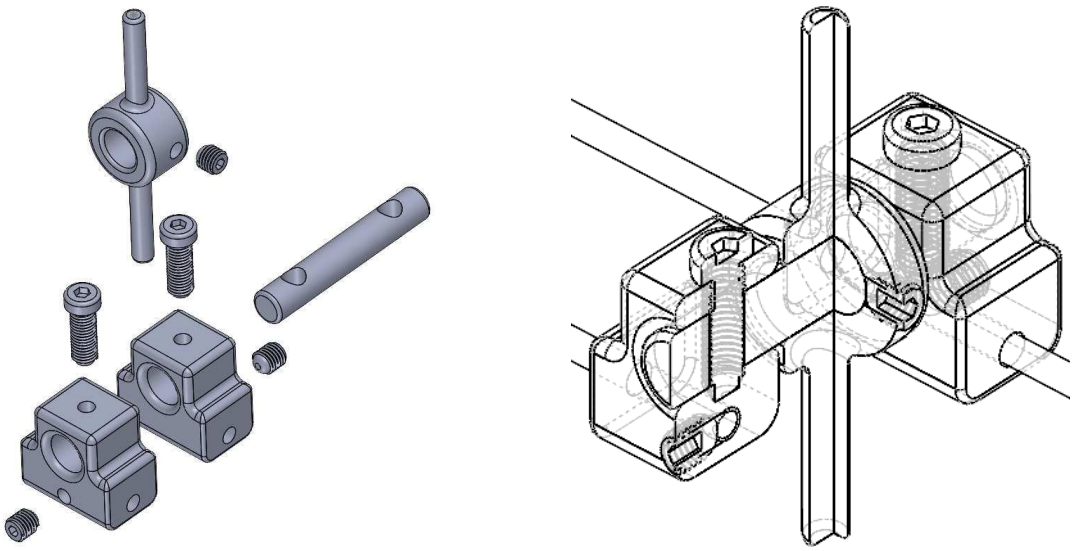

a) b)

Figure 4.6 - Representation of the fixation system with all components: a) Exploded view; b) Sectional model, with Kirschner wires.

Cutting Regulation System

The cutting regulation system, shown in Figure 4.7, is composed by three bars connected by an adjustable and fixation radial knurled between the components and guide components inserted in each of the bars.

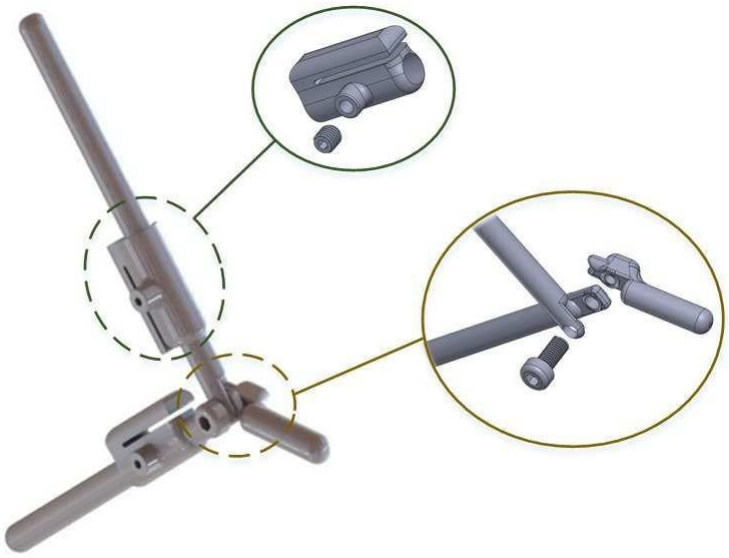

Figure 4.7 - Representation of the cutting adjustment system, with expansion of the connection/adjustment area of the adjustment bars with knurled and the guide components.

The guide component inserted in each of the long bars allows the defining of the longitudinal position (L_c) and radial variation (β). The screw-based fastening system locks the guide member together with the bar. The end of the short bar comprises a guided position with the definition of the virtual center of the cut. A set of discrete angles between the two long bars can be defined (α). Figure 4.8 shows the exposed concept in more detail.

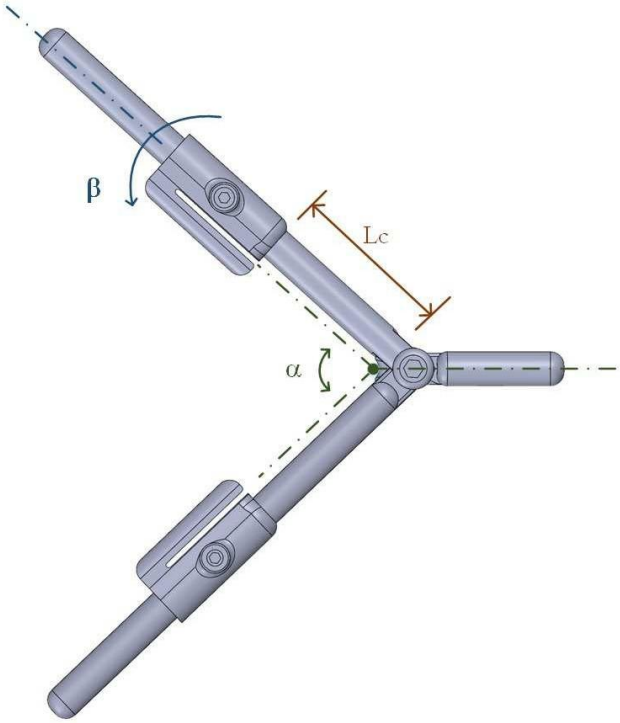

Figure 4.8 - Angle representation of the cutting adjustment system.

Angular Adjustment System

The angular adjustment system is composed with two main arc components, namely a principal arc and a secondary or clamped arc. The two arcs are fixed together with four adjusted screws (Figure 4.8). The two arcs also have a set of rubber O-rings to provide the grip with the bars from the cutting regulation system.

a) b)

Figure 4.9 - Representation of the angular adjustment system: a) Assembly; b) Exploded view.

Figure 4.10 shows the two arcs assembled with the bars. The concept of use the O'rings was chosen to provide an easy way to adjust and clamp the bars between the arcs.

Figure 4.10 - Representation of the two arcs assembled with the bars.

The angular adjustment system is anchored to the fixation system. Figure 4.11 presents a perspective and detailed view of this concept. This system allows cutting with lengthening or shortening, manipulating the φ angle (adjustable around y), and cutting with planterization, adjusting the γ angle (around x).

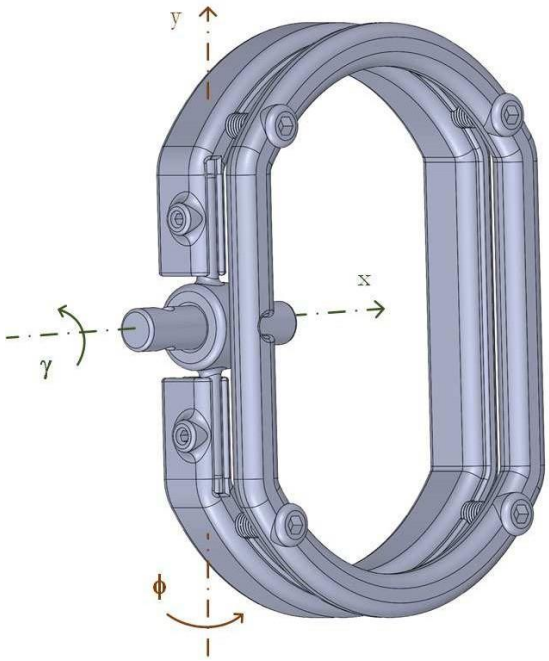

Figure 4.11 - Representation of the adjustment system anchored in the fixation rotation guide.

Drilling Guidance System

The drilling guidance system is composed by a bar with a particular screw to be easily inserted and blocked into the long arc of the angular adjustment system an adjustable component will serve as a guide for the drilling process. Figure 4.12 shows the components of the drilling guidance system and its assembling in the long arc, together with the drill for a better understanding.

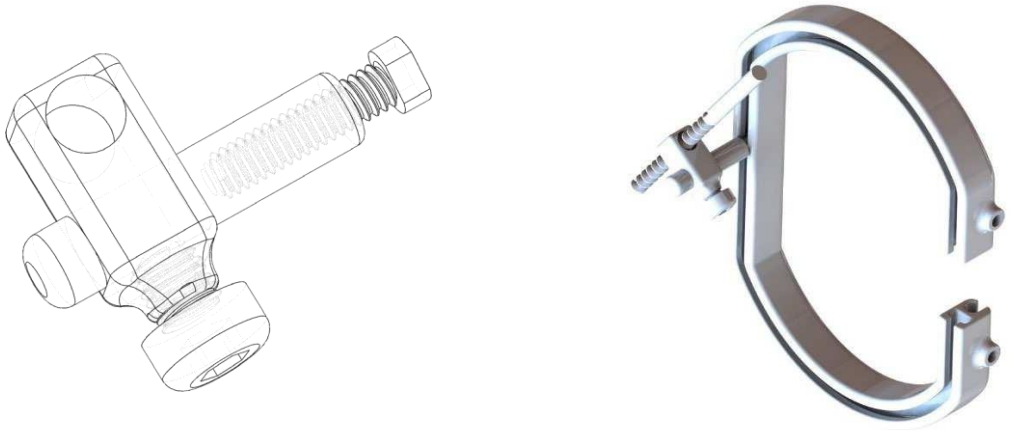

a) b)

Figure 4.12 - Drilling guidance system: a) Representation of the drilling guidance system; b) System coupled to the main guide of the angular adjustment system, with drill.

As can be observed in the Figure 4.13, the drilling guidance system has three degrees of freedom to provide the adequate definition of the drill position. First, the nut component can move along the rail in the long arc (C). Second, the guide component

can be longitudinally adjusted (L_D) as also angularly adjusted (ρ). The rotation of the bar around x will promotes the grip into the rail.

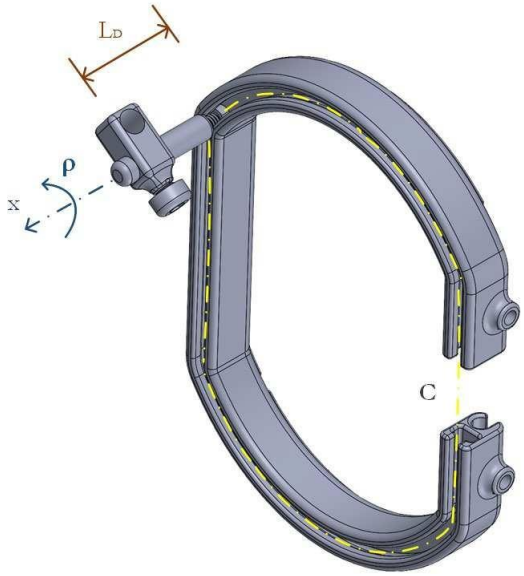

Figure 4.13 - Representation of the rendered model of the coupled drilling system, with longitudinal and rotational adjustments.

4.1.2 Device Materials and Prototyping

The idea concerning the device prototype was to implement the possibility to use materials that can be manufactured with easy processes, allowing short series of the device. It must be pointed out that the final objective is to use the device in surgical conditions, and it would not be an invasive system, since only the Kirchner wires, the blade and the drill will have a direct contact with the bone. The device will be only a support system to guide the blade and the drill.

Following these considerations, the device has been developed supporting the possibility to implement the additive manufacturing technologies to the main components. Then, the selection of materials and technologies used were based on this project considerations.

Polyethylene Terephthalate (PET)

The Polyethylene terephthalate (PET) was chosen to produce main components. The material is one of the most used polymeric materials in the health area (Swar, et al., 2017), mainly due to its advantages, which include high strength and toughness, good resistance to abrasion and heat, low creep in high temperatures, good chemical resistance and excellent dimensional stability. Also, PET has excellent wear resistance, low moisture absorption and is very durable.

Infarmed (National Authority for Medicines and Health Products I.P) considers that the medical devices covered by Directive n.º 93/42/EEC, in its current wording, transposed into national law by Decree-Law n.º 145/2009 of 17 June, are divided into four risk classes considering the vulnerability of the human body and the

potential risks arising from technical design and manufacture. This device is part of class IIa medical devices - medium risk. This classification depends on four fundamental points relating to the devices (Infarmed, 2023): a) Duration of contact with the human body, which can be short-term, long-term or temporary (the case of this device); b) Invasiveness of the human body; c) Anatomy affected by use; d) Potential risks arising from technical design and manufacturing.

Recent studies on the antibacterial properties of PET have shown that several surface modification technologies have been used to limit and/or prevent bacterial contamination of PET, namely functionalization, grafting, surface topography modification, and coating. The methodologies are illustrated in Figure 4.14.

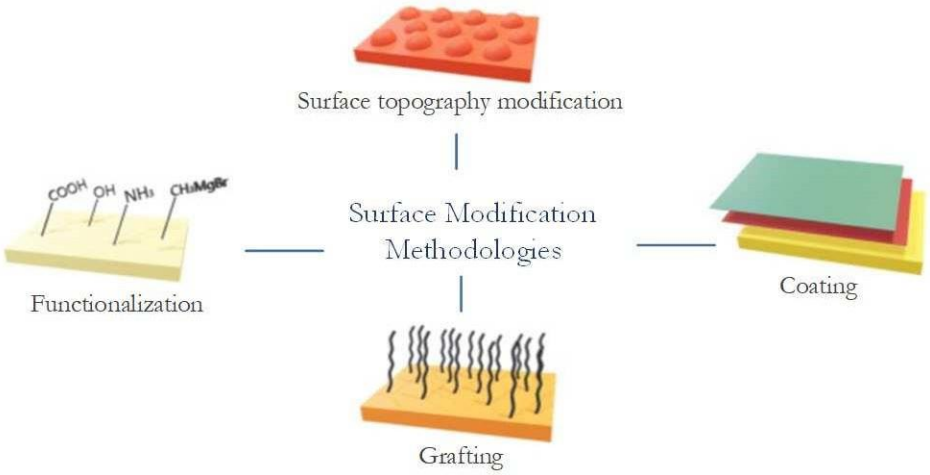

Figure 4.14 - Surface modification methodologies used to develop antibacterial PET surfaces. Adapted from (Çaykara, Sande, Azoia, Rodrigues, & Silva, 2020).

Current developments show that the treated PET surface has significantly higher antibacterial activity than the original.

However, potential bacterial resistance, cost-effectiveness, the durability of the modification, and the possible toxic effects of antibacterial agents on the environment, must be considered when choosing the most suitable modification approach for the anticipated PET products. Bearing that it is not an invasive device in the human body, it becomes more advantageous in terms of cost/benefit than a disposable device (Çaykara, Sande, Azoia, Rodrigues, & Silva, 2020).

Silicone Material

For the rubber profile, regular silicone was chosen, with 60SH A hardness and service temperature of 200ºC. This chosen material is in accordance with FDA (Food and Drug Administration) certification, following the requirements for medical devices (Sove, 2023).

Metallic Accessories

The components are assembled using M3 screws, M3 inserts, and M3 studs, as shown in Figure 4.15. To all this component, the AISI 316 L stainless steel was considered. It is a variation of AISI 316 stainless steel with reduced carbon content,

which helps to increase resistance to intergranular corrosion, which has as properties excellent resistance to corrosion in corrosive environments, including exposure to acids and alkaline solutions, high tensile and fatigue strength, high ductility, which means it can be easily shaped in various forms. The AISI 316 L is a well-known material for several application in surgical.

a) b) c)

Figure 4.15 - Representation of the connection components: a) Studs; b) Screws; c) Inserts.

Production of Components

The choice of materials led to adopt the manufacturing process, commonly known as 3D printing, which consists of an additive manufacturing process which generates very little waste, just on the supports. The entire additive manufacturing process was implemented using an Original Prusa® i3 MK3S+ 3D printer and the respective PrusaSlice printer software, available at Applied Biomechanics Laboratory (LBA). The printer was used with a 0.25 [mm] nozzle, with a precision of 0.1 [mm], to make the part as accurate as possible. Figure 4.16 and 4.17 shows a snapshot of one of the device's components and an image of this printer, respectively. Print parameters have been optimized to avoid fractures due to saw vibrations (massive print, 100% filling).

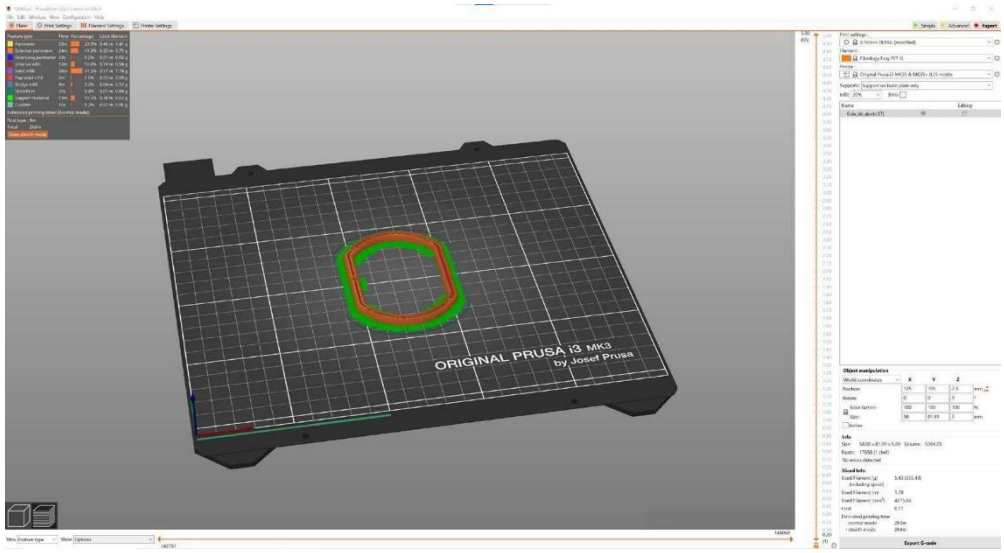

Figure 4.16 - Preparation of a part on the PrusaSlicer.

Figure 4.17 - Visualization of a printing moment.

Final Prototype

Based on what was explained above in this chapter, it was possible to obtain the final prototype, shown in Figure 4.18, produced with PET, silicone and AISI 316 L stainless steel.

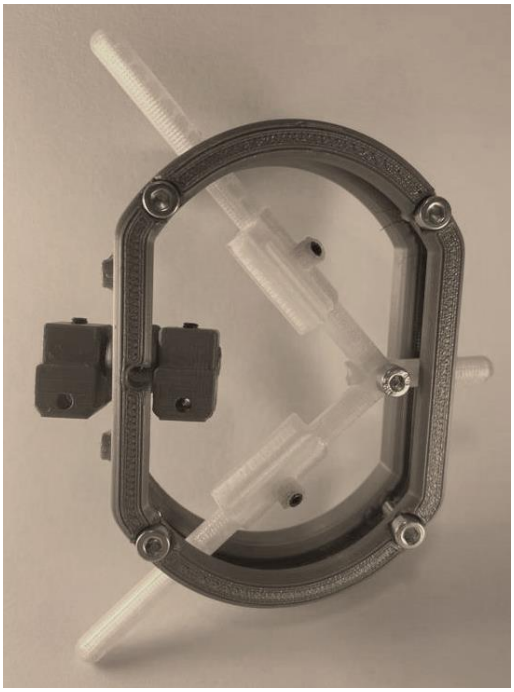

Figure 4.18 - Final prototype.

4.1.3 Device Prototype Assembly – a Perspective for Surgery Conditions

The main objective of the device is to be used in surgery conditions, to help and improve the Chevron surgery, as explained. Then, it would be important to understand the perspective of use the system in these conditions, knowing that the surgical behavior have particularities that must be considered. From the perspective of using the device in surgical conditions, all the components must be well sterilized before its use.

Step 1 – Pre-Preparation

The use of the system involves a pre-preparation environmental situation. As a first step, the instrument nurse at the surgery site should mount the device with the position defined by the surgeon. Then, the device will be assembled as show in Figure 4.18.

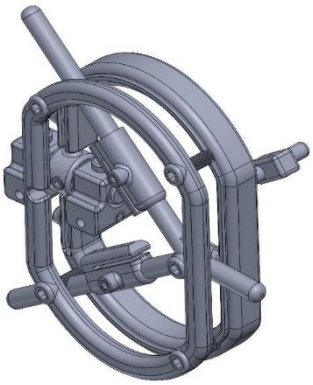

Figure 4.19 - Representation of how the device arrives in the operating room.

Step 2 – Device Fixation

When performing the procedure, the surgeon marks where he wants the cuts to join in the bone and, aligning the adjustment system of the device with the marking point where the cuts join, the Kirschner wires are placed, as shown in Figure 4.20a), fixing the device to the wires and the wires to the bone correctly. In this way, the device is correctly positioned and anchored for guided support to the cuts can be made, as shown in Figure 4.20b).

a)

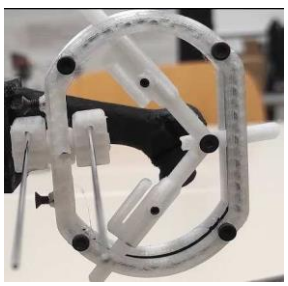

b)

Figure 4.20 - Representation of some of the stages of the surgical process: a) Fixed Kirschner wires; b) Fixation of the device on the wires

Step 3 – Cut

Then, the surgeon proceeds to cut the bone with the help of the guides, allowing the necessary precision for the procedure (Figure 4.21).

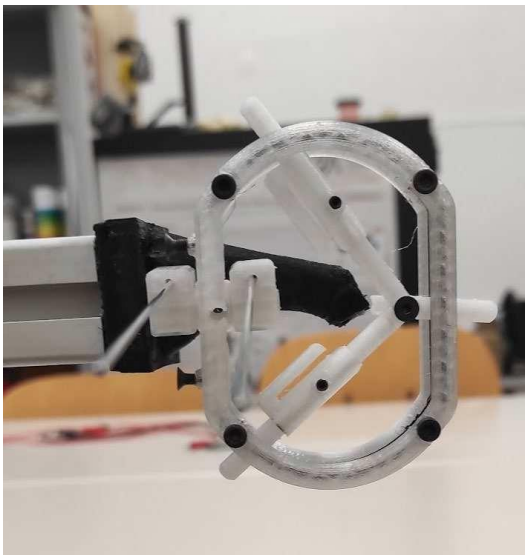

Figure 4.21 - Representation of the metatarsal cutting procedure.

After cutting, the bone segments are repositioned. This procedure is done manually. After this repositioning, the bone segments connection is stabilized, which is done by placing two union screws. To ensure screw tightening alignment, the drill guide is positioned and oriented correctly. The surgeon also performs this procedure. This is how the guided tightening is done with screws that unite the two parts of the bone.

After the surgical cutting and stabilization procedure, the Kirschner wires are removed from the bone, and the device is removed.

Then, the usual closure of soft tissues opened for surgery is performed.

5 DEVICE EXPERIMENTAL EVALUATION

The device prototype was tested in a laboratory context by an orthopedist. To implement the experimental tests, the bone model exposed in this chapter was considered and manufactured as similar as possible with the real bone. After, an experimental setup was defined, and the tests performed. This chapter explains the methodology considered to obtain the bone specimens, the experimental protocol defined, and tests executed, as its results. The main objective is to obtain the first conclusions concerning the behavior of the device.

5.1 Bone Model

The metatarsal bone model is the most important to check the device as it will be used for cutting tests. The material properties for obtaining a real model must be like those of cortical and trabecular bone. According to (Paulino, Roseiro, Balacó, Neto & Amaro, 2022), the cortical bone has, on average, an Elasticity Modulus of 0.7 GPa and the trabecular zone has an average of 17 GPa.

The methodology used to obtain a reliable model considers the preparation of the bone with only its cortical component and produce this element with additive manufacture. After, the trabecular zone must be injected to fill out the trabecular zone. To have the bone stable in carrying out the experimental tests, an anchorage zone was defined at one of the extremities. The Figure 5.1 shows the bone model before and after preparation and it can be observed two holes in the extremities to perform the injection of material, as the fixation extremity.

a) b)

Figure 5.1 - Representation of the bone model: a) Original bone model; b) Bone model prepared.

Considering the material possible to be used, the Polyethylene Terephthalate Carbon Fiber, with a Modulus of Elasticity of 9 GPa and Tensile Strength of 80 MPa, was selected to represent the cortical regions. For the trabecular regions, the Soudan, ultra-expansive foam of PU (Polyurethane) was selected.

The cortical model was first prototyped using FFF with the Prusa MK3S+ equipment, with a 0.6 nozzle, 0.3 mm precision, choosing the following features based on experience: Filling = 60%; Nozzle temperature = 265º; Bed temperature = 90º. After, the PU foam was inserted to obtain the trabecular regions. Figure 5.2 shows the first preparation of the bone model with lateral support.

a) b)

Figure 5.2 - First bone preparation: a) Entire model; b) Sectioned model.

5.2 Experimental Setup and Protocol

The preparation of the experimental tests involved the use of the bone specimens and the material normally used in surgical procedures. Figure 5.3 presents the components and materials used in the experimental tests, namely a support system to fix the metatarsal bone model, the developed and assembled device, two 1.5 (mm) Kirschner wires, the cutting blade (Hestia XinSheng from 4a Medical), and the saw (Shanghai XinSheng photoelectric).

The protocol to perform the experimental tests and data acquisition was defined by the team and can be described as follows:

1.Fixation of the bone support system;

2.Adjustment of the device according to the intended cutting angles;

3.Marking the connection point of the cuts;

4.Positioning adjustment, considering the previously marked point;

5.Fixation of the Kirschner wires in the metatarsus;

6.Fixation and stabilization of the device on the Kirschner wires;

7.Performing the cuts with the saw;

8.Metatarsal head adjustment;

9.Drilling guide adjustment;

10.Drilling/fixation of the two parts of the bone;

11.Removal of the device;

12.Close soft tissue.

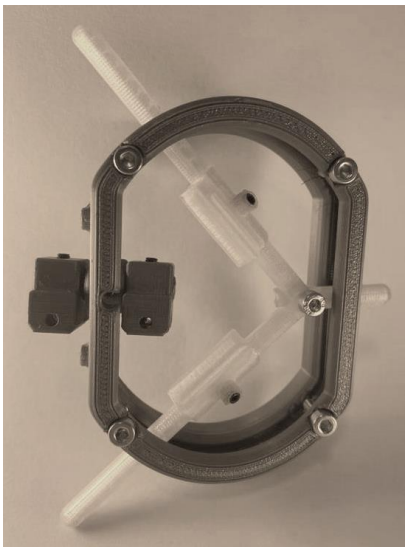

a)

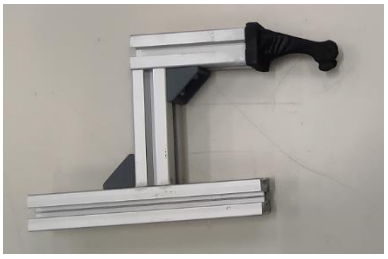

b)

c)

d)

e)

Figure 5.3 - Components and material used to carry out the tests: a) Device; b) Bone support system; c) Cutting blade; d) Kirschner wires; e) Saw.

5.3 Experimental Tests

A total of four tests were defined by the orthopedists, each one with different positional adjustments associated with the Chevron technique and different angles, representing (Figure 5.4): a) Metatarsal Plantarization (40º up, 35º down); b) Stretching (35º up, 40º down); c) Plantarization + Stretching (35º up, 60º downwards); d) Large plantarization + shortening (50º upwards, 60º downwards).

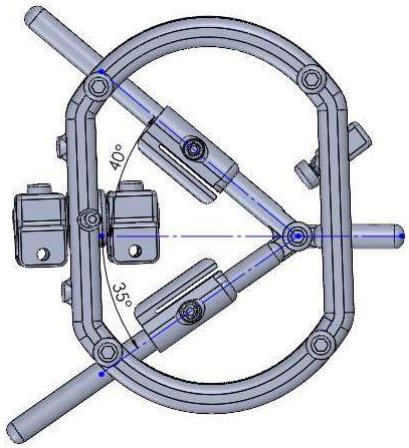

a) 40º up - 35º down

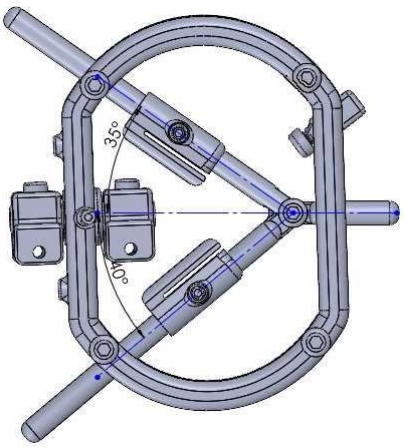

b) 35º up - 40º down

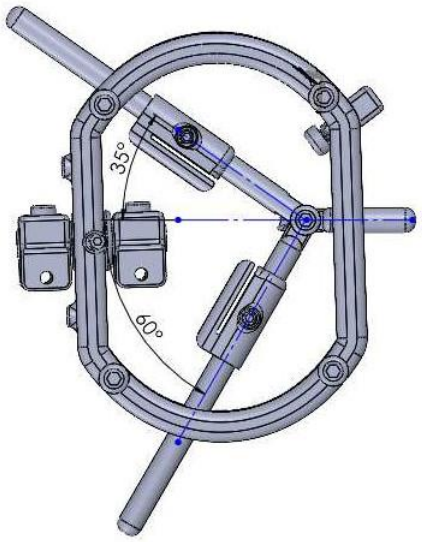

c) 35º up - 60º downwards

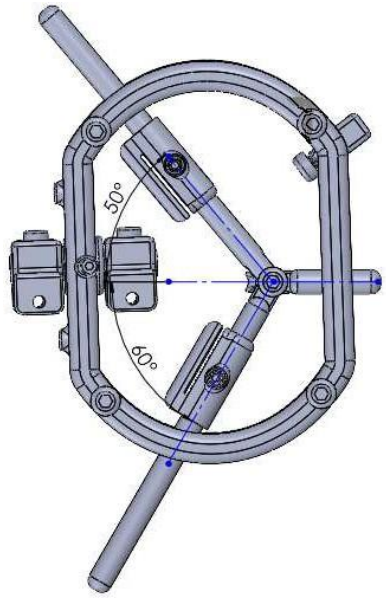

d) 50º up - 60º downwards

Figure 5.4 - Representation of cutting angles: a) 40º up, 35º down; b) 35º up, 40º down; c) 35º up, 60º downwards; d) 50º upwards, 60º downwards.

All the experimental tests were performed by an experienced orthopedist, a member of the research team. As a first step, the Kirschner wires were fixed in the bone, similarly to the routine procedure in the Chevron Osteotomy. For this purpose, the

part of the device to be set in the Kirschner wires was used to guarantee the distances and alignment of the wires. After, the device is fixed in the Kirschner wires, so it is possible to make the cuts with the aid of the guides. In this step, before fixation, the device was adjusted according to the intended cutting position.

The Figure 5.5 shows the orthopedist performing part of the experimental test in a bone specimen, namely the position of the device, a moment of cutting and a moment of fixation the screw.

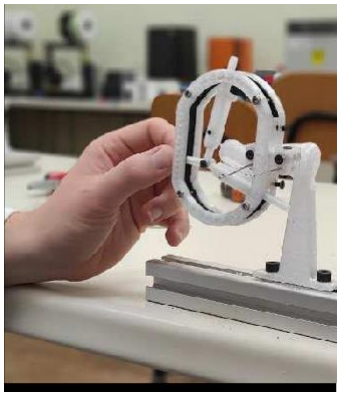

a)

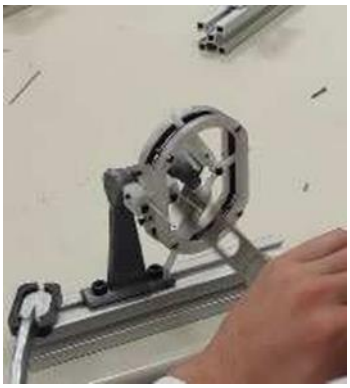

b)

c)

Figure 5.5 - Visualization of some procedures make by the orthopedist: a) Position of the device; b) Bone cutting; c) Fixation of the screw.

5.4 Results and Discussion

Figure 5.6 shows the bones after the cuts. First, the observation of the cutting surfaces was considered and analyzed. After, the measure of the cut angle was implemented with an angle measuring instrument, to compare the result with the defined for the test.

The results obtained show well-defined cuts with deviations of 2º in the uppercut and 3º in the lower one, in the case of metatarsal planarization, deviations of 4º

superior and 3º inferior, in the case of stretching, deviations of 2º in the uppercut and 1º in the lower cut, in the case of plantarization + stretching and deviations of 2º in the uppercut and 3º in the lower cut in the case of large plantarization + shortening. Also, all the cutting surfaces presents a good definition. Figure 40 shows the visualization of the cuts performed in the tests.

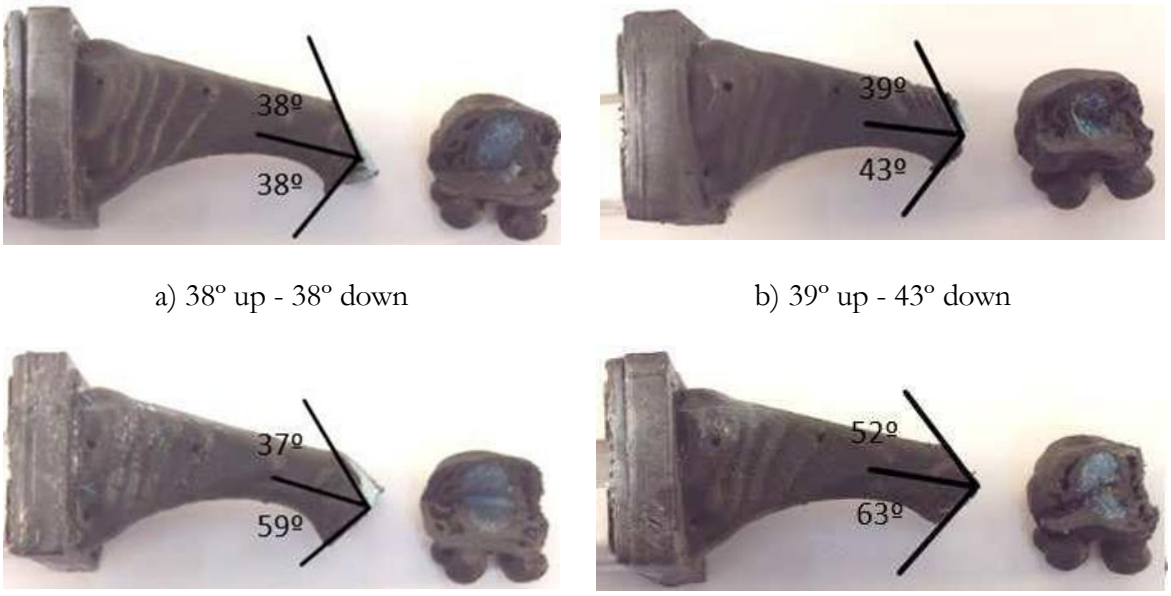

a) 38º up - 38º down

b) 39º up - 43º down

c) 37º up - 59º down

d) 52º up - 63º down

Figure 5.6 - Visualization of the cuts performed in the tests: a) Metatarsal Plantarization (38º upwards, 38º downwards); b) Stretching (39º upwards, 43º downwards); c) Plantarization + Stretching (37º upwards, 59º downwards); d) Large Plantarization + Shortning (52º upwards. 63º downwords).

The device showed adequate resistance and rigidity to support the execution of cuts, demonstrating that it can function as a support and guidance system. It should also be noted that, after the cut performed in each of the tests, the general state of the device was observed, which was in the proper conditions. However, it should be noted that the purpose of producing the device with these materials and manufacturing techniques is in line with its single use.

Thus, it can be stated that, for the four tests performed, the device met the objectives defined in each of the tests performed. In fact, the first experimental results suggest that the device can represent a significant advance to assist in the implantation of the Chevron Osteotomy. However, it is expected that further experimental and clinical testing (with cadaver testing of the device on the waiting list) will validate the device's effectiveness and assess its impact on long-term patient satisfaction and functional outcomes.

6 CONCLUSIONS AND FUTURE DEVELOPMENTS

The presented work involved the development of a new biomechanical device to support the Chevron osteotomy. One of the important aspects of this project was the fact that it involved a completely different disciplinary domain than usual for the author. This aspect forced research out of the box and promoted leaving the school doors and teamwork with orthopedic doctors, having been highly motivating and a boosting factor for the skills acquired in the course of this work.

The implementation of the work leads to carry out several methodologies considered relevant in its context, and the author wants to let pointed out some relevant aspects. One of the aspects was the bibliographic research. This part of the work was relevant, leading to the study the anatomy of the human foot, the HVA pathology and identification of the Chevron Osteotomy surgical procedure. Also, the identification of the state of art concerning the devices to support the Chevron Osteotomy was important, and shows only one device, with several limitations.

6.1 First Conclusions

Bone Model

The development of a 3D model of a metatarsus bone was an important step. The bone was obtained from a CT scan and produced with a mix methodology, based on additive manufacturing for the cortical region, followed by the injection of material to fill out the trabecular region.

Device Development

The device was developed with 3D CAD methodology. The concept leads to a first prototype, produced, and tested. After, an iterative optimized process was implemented, arriving at the final geometry exposed. This process undergoes verifying the existence of a link between geometry, functionality, production, and simplicity of use. This link was obtained on two relevant levels: a) Clinical compliance, emphasizing the execution of the Chevron osteotomy technique; Ease of production through additive manufacturing, with a design that simplifies the 3D printing process.

First Experimental Tests

Considering the device prototype and the bone model, some experimental tests were implemented, based on the implementation of the Chevron Osteotomy. These first experimental tests, performed by and experimented Orthopedist, shows interesting results, with well-defined cuts. The necessary guidance and stabilization were observed, showing that the device can leads to carrying out the surgical procedure in a much more precise way.

It is important to reinforce that the concept behind the development of this device involved the use of additive manufacturing technologies and the use of materials and components that can be used in a surgical environment. This aspect can represent an added value or a difficulty in the certification of this type of device. Despite the author's concern with this aspect, only future steps, already under implementation and written below, will be able to answer these questions.

6.2 Future Works

Some improvements concerning the optimization and test of the device are in implementation.

Bone Model

One of improvements for better future experimental tests is the artificial bone model. This improvement in already in implementation and is based on additive manufacturing with multi-materials. The PET Carbon Fiber was selected for the cortical region, which has a Modulus of Elasticity of 9 GPa and Tensile Strength of 80 MPa and the TPU (Thermoplastic polyurethane) Carbon Fiber, which has a Modulus of Elasticity of 1450 MPa and Tensile Strength of 65 MPa, was selected for the trabecular region. The first models in production, obtained from this methodology can be observed in Appendix B.

In a subsequent phase, it is intended to conduct the device tests with the new bone models to obtain the cutting and drilling performing as realistic as possible.

Device in Aluminum

As exposed, the device was developed to follow a production with additive manufacturing and a single use. As a future step, it is intended to get a reusable instrument, requiring only new sterilization after each use. This can be obtained with the use aluminum, given that the mass of the device is a relevant aspect in the developed concept, as its anchorage in the Kirschner wires.

After researching the existing literature, aluminum 6061 was chosen as suitable for machining this device. The 6000 series is one of the most versatile and cost-effective (Ltd., 2023). Aluminum 6061 has a tensile strength of 124-290 MPa and a yield strength of 276 MPa; in addition to being considered one of the most accessible materials to anodize, an essential characteristic of the optimized device (Co., 2023). The anodization procedure controls and forces the oxidation of aluminum (in alumina) so that the oxidation layer can be between 0.5 μm and more than 100 μm. In the context of biocompatibility and ISO-10993, the anodized surface provides a barrier against aluminum (Trousil, 2013) (Danco, 2023). This device needs to be sterilized but will not meet soft tissue or bone. Only the Kirschner wires will be in direct contact with the bone.

To produce the device in aluminum it will be necessary to use subtractive manufacturing technologies, with a suitable machining center. Then, it will be necessary to adjust the components geometry to meet the machining requirements. This work is already developed, and the new geometry is exposed in the appendix C.

Device Tests Improvement

It is expected that the tests to be carried out with the artificial bone model described above will contribute to collecting more complete data on the effectiveness of the device. However, it will be important for the validation of the use of the device to carry out more experimental tests and in conditions closer to reality. Thus, it is expected to improve the experimental setup for tests and conduct them with two more types of bone; a) Certified artificial bone, from the Sawbones brand; b) Cadaveric bone.

The use of cadaveric bone will require the use of a bone bank and the authorization from an ethics committee.

Tt is also important to refer that the intention is to implement the new tests with several orthopedists, to obtain a broader spectrum of evaluation by the surgeons who usually perform this type of surgical procedure.

6.3 Some Outcomes

This project was developed in the Instituto Superior de Engenharia de Coimbra, Applied Biomechanics Laboratory, in conjunction with an orthopedist. Carrying out this work allowed the acquisition of essential skills in the context of training in mechanical engineering, with the design, execution, and manipulation of mechanical components and equipment. In addition to the prototype presented, during the work carried out, it was possible to participate in a set of actions that allowed the dissemination of the ongoing project and the registration, through a publication, of the results obtained. Also, in this domain, learning was relevant. These activities and publications are listed below:

National Patent Application

The work developed was submitted by The Polytechnic Institute of Coimbra to obtain a provisional application for a National Patent:

M. Santos, E. Cortesão Seiça, P. Carvalhais, and L. Roseiro (inventors), Dispositivo de fixação e regulação para osteotomia de Chevron, INPI reference number GCF3190169.

X CNB 2023 – Oral Presentation

The developed work was submitted and accepted for oral presentation in the X Congress of the Portuguese Society of Biomechanics, which took place at the Center

for Arts and Spectacles, in Figueira da Foz, on May 5th and 6th, 2023. The participation in the Congress and oral work presentation was done, with title "Fixation and Adjustment Device for Chevron Osteotomy" and was registered in the Congress Proceedings.

X CNB 2023 – Winner of Prize Better Prototype

During the congress, the developed device participated in the competition for the best prototype, winning first place.

Springer Book - Proceedings of the 10th Congress of the Portuguese Society of Biomechanics

After the X CNB Congress, a long version of the work was submitted to integrate the special edition of Springer – "Proceedings of the 10th Congress of the Portuguese Society of Biomechanics.". After the revision process, the work was accepted:

M. Santos, E. Cortesão Seiça, P. Carvalhais, and L. Roseiro (2023). Fixing and Adjusting Device for Chevron Osteotomy.

ICCB 2023 - X International Conference on Computational Bioengineering

Participation in the ICCB Congress, Vienna, Austria, September 20 - 22, 2023. The submitted work ("Development of a Biomechanical Device to Support the Fixation and Adjustment for Chevron Osteotomy"), after review and acceptance will be orally presented and registered in the Congress Proceedings.

BIBLIOGRAPHY

Bascarević, Z. L., Vukasinović, Z. S., Bascarević, V. D., Stevanović, V. B., Spasovski, D. V., & Janicić, R. R. (2011). Hallux valgus. *Acta Chir Iugosl*. Retrieved from https://pubmed.ncbi.nlm.nih.gov/22369028/

Çaykara, T., Sande, M. G., Azoia, N., Rodrigues, L. R., & Silva, C. J. (2020). Exploring the potential of polyethylene terephthalate in the design of antibacterial surfaces. *Med Microbiol Immunol*, 363-372. doi:10.1007/s00430-020-00660-8

Co., S. T. (2023, julho 14). *6061 vs 6063 Aluminum: What's the Difference Between?*

Retrieved from China Shenzhen Tuofa Precision CNC Machining Manufacturer: https://www.tuofa-cncmachining.com/tuofa-blog/6061-vs-6063- aluminum.html

Cohen, J. C., Richardson, G., & Fernandes, R. M. (2010). Surgical treatment of moderate to severe hallux valgus with distal chevron. Retrieved from file:///C:/Users/Utilizador/Downloads/Tratamento+cir%C3%BArgico+do+h%C3%A1lux+valgo+moderado+%C3%A0+grave+por+meio+da+osteotomia+distal+tipo+chevron+associado+%C3%A0+libera%C3%A7%C3%A3o+distal+de+partes+moles.pdf

Danco. (2023). Anodizing Considerations for Medical Devices Machined from Aluminum. Retrieved from chrome-extension://efaidnbmnnnibpcajpcglclefindmkaj/http://www.danco.net/pdf-downloads/medical-devices.pdf

Infarmed. (2023, julho 14). *Classificação e fronteiras*. Retrieved from Infarmed:https://www.infarmed.pt/web/infarmed/entidades/dispositivos-medicos/classificacao-e-fronteiras

Jahss, M. (1991). Disorders of the Hallux and the First Ray. In *Disorders of the Foot and Ankle: Medical and Surgical Management* (2ª ed., Vol. II, pp. 943-1073). W. B. Saunders Company.

Kenhub. (2023, julho 14). *Bones of the foot*. Retrieved from Kenhub:

https://www.kenhub.com/en/study/foot-bones-and-ligaments

Kenhub. (2023, julho 14). *Joints and ligaments of the foot*. Retrieved from Kenhub: https://www.kenhub.com/en/study/ligaments-of-the-foot

Kenhub. (2023, julho 14). *Muscles of the foot*. Retrieved from Kenhub: https://www.kenhub.com/en/study/muscles-foot

Lerat, J.-L. (2011). Cheville-Pied: L'Hallux Valgus. In S. d. Centre Hospitalier Lyon-Sud,

Traumatologie Orthopédie (p. Cap. 6).

Ltd., M. F. (2023). *Choosing An Aluminium Alloy for Anodising*. Retrieved from Metal Finishings Ltd.: https://metalfinishingsltd.co.uk/articles/best-anodising-alloy/

Martins, P. P. (2013, 3). Hallux valgus : estratégia cirúrgica. Retrieved from http://hdl.handle.net/10316/85684

Nguyen, J., Sullivan, M., Alpuerto, B., Mueller, S., & Sly, N. (2019). A radiographic analysis of the abnormal hallux interphalangeus angle range: Considerations for surgeons performing Akin osteotomies. *Journal of Orthopaedic Surgery*. doi:10.1177/2309499019841093

Nix, S., Smith, M., & Vicenzino, B. (2010). Prevalence of hallux valgus in the general population: a systematic review and meta-analysis. *Journal of Foot and Ankle Research*. doi:https://doi.org/10.1186/1757-1146-3-21

Paulino, M., Roseiro, L., Balacó, I., Neto, M., Amaro, A. (2022). Evaluation of Bone Consolidation in External Fixation with an Electromechanical System. Aplied Sciences. https://doi.org/10.3390/app12052328

Perera, A., Mason, L., & Stephens, M. (2011). The Pathogenesis of Hallux Valgus. *The Journal od Bone Joint Surgery*, 1650-1661. doi:10.2106/JBJS.H.01630

pied, C. d. (2023, julho 14). *Hallux Valgus or Bunion*. Retrieved from Geneva Foot Center: https://www.centrepiedgeneve.ch/en/hallux-valgus/

Sharma, J., & Aydogan, U. (2015). Algorithm for Severe Hallux Valgus Associated With Metatarsus Adductus. *Foot & Ankle International*, 1499-1503. doi:10.1177/1071100715593799

Sorrisos, O. Q. (2023, julho 14). *Como corrigir os Joanetes (Hallux Valgus)?* Retrieved from Ortopedia Universo Sénior: file:///C:/Users/Utilizador/OneDrive/Ambiente%20de%20Trabalho/Tese/Pesquisa/Importante/Como%20corrigir%20os%20Joanetes%20(corretor%20joanetes%20Hallux%20Valgus)_.html

Sove. (2023, July 14). *Perfis Borracha Silicone Normal*. Retrieved from Sove: https://www-tecnicos/perfis/perfis_borracha_silicone/perfis-borracha-silicone-normal/?_gl=1*hjm13k*_up*MQ..*_ga*MTk5MDA4NjE2My4xNjg5MDM0MzMw*_ga_ENTQV0M36K*MTY4OTAzNDMyNi4xLjEuMTY4OTAzNDM1MS4wLjAuMA..*_ga_SLY38DTR68*MTY4OTAzNDMyO

Swar, S., Zajícová, V., Rysová, M., Lovetinská-Šlamborová, I., Voleský, L., & Stibor, I. (2017). Biocompatible surface modification of poly(ethylene terephthalate) focused on pathogenic bacteria: Promising prospects in biomedical applications. *Journal of Applied Polymer Science*. doi: https://doi.org/10.1002/app.44990

Trousil, D. (2013, julho 14). *Is Anodized Aluminium Biocompatible?* Retrieved from StarFish Medical: https://starfishmedical.com/blog/anodized-aluminium-biocompatible/

Zixuan, L., Fengqi, Z., Yansen, L., Xiaomeng, W., & Shoujia, L. (2020). *Patent No.*

CN211381609U.

APPENDICES

Appendix A - Geometric details of device components

All the mechanical components and geometric details and dimensions of the device can be found in this appendix.

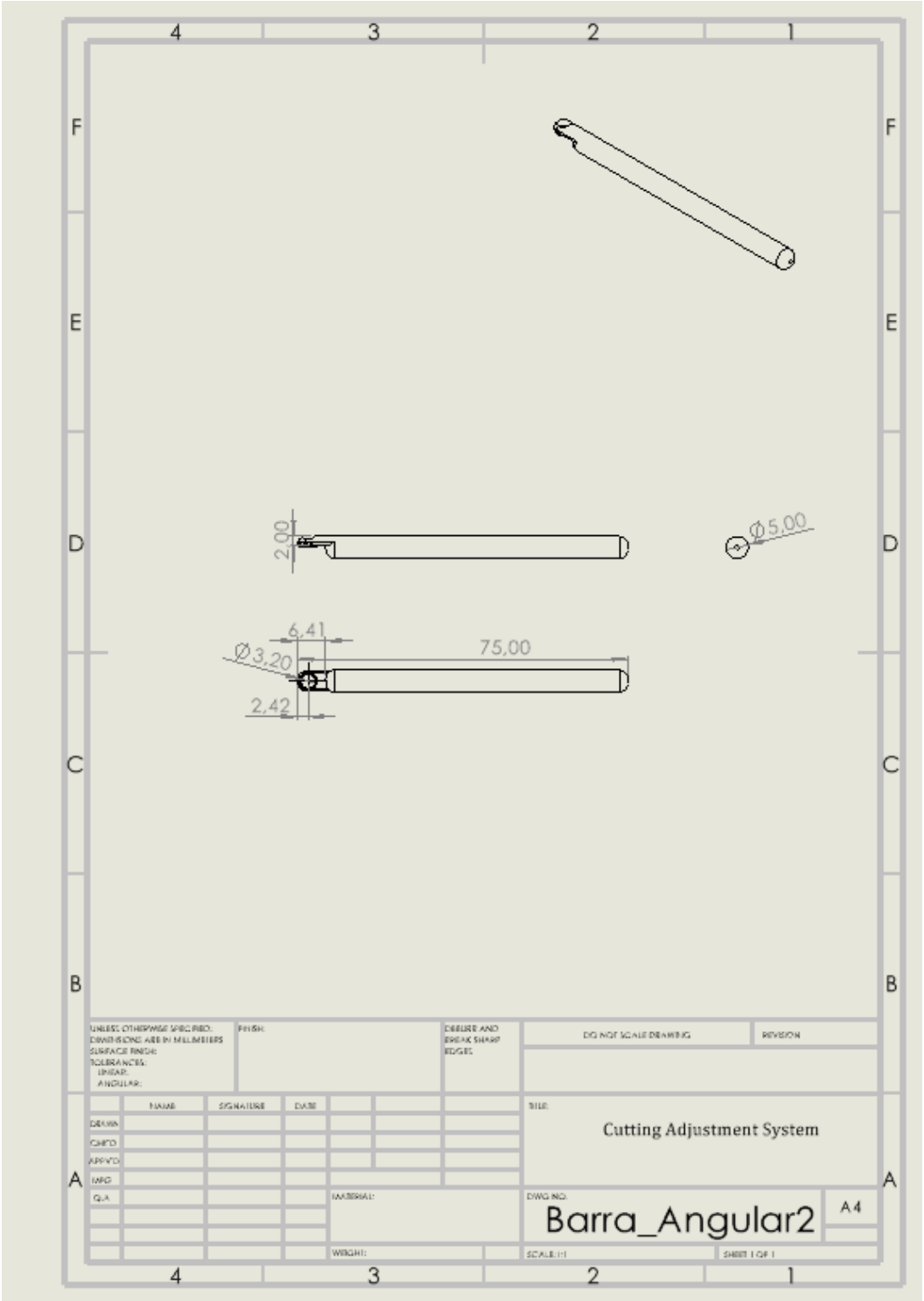

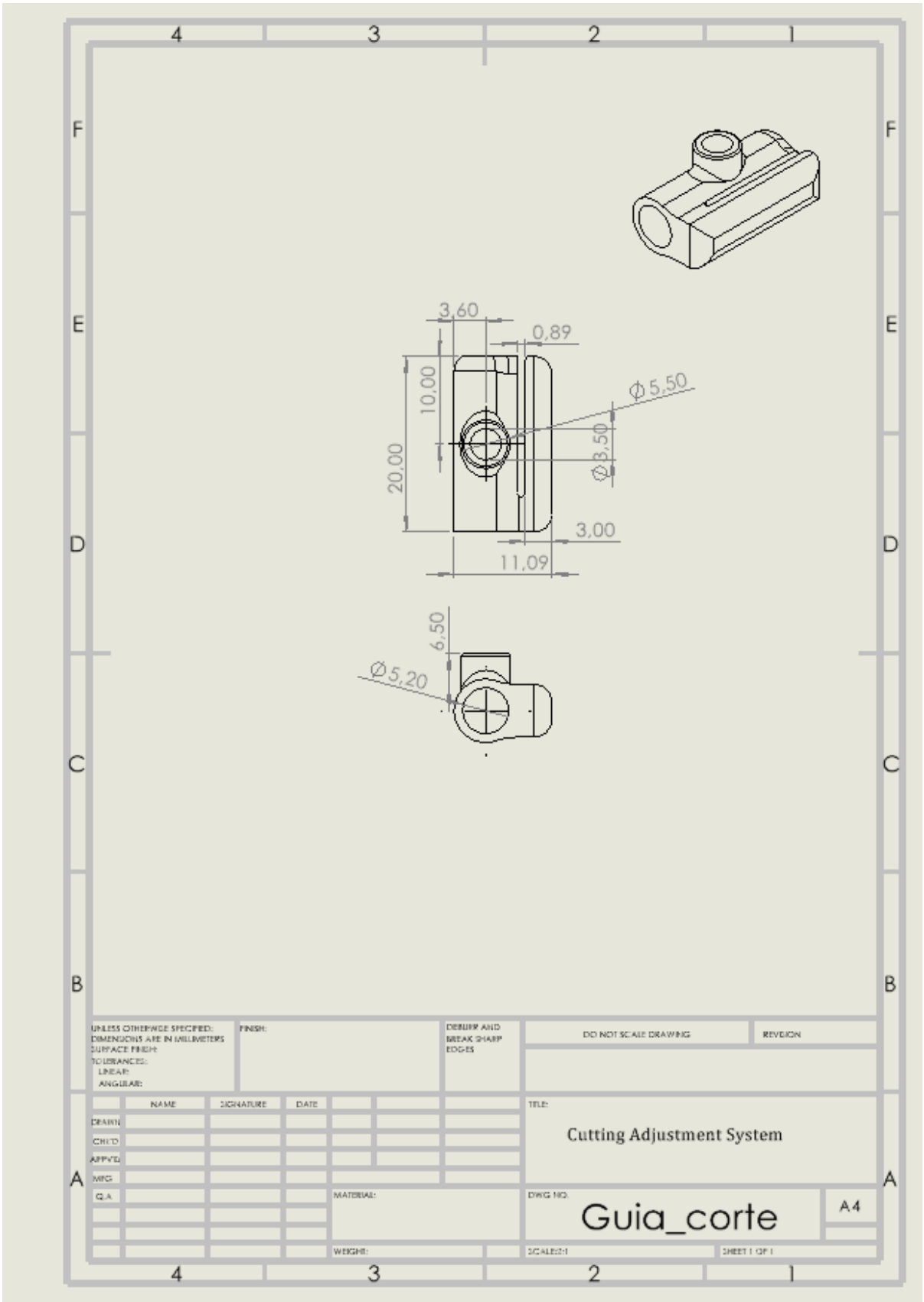
3,60
0,89
10,00
20,00
Ø5,50
Ø3,50
3,00
11,09
6,50
Ø5,20
UNLESS OTHERWISE SPECIFIED:
DIMENSIONS ARE IN MILLIMETERS
SURFACE FINISH:
TOLERANCES:
LINEAR:
ANGULAR:
FINISH:
DEBURR AND BREAK SHARP EDGES
DO NOT SCALE DRAWING
REVISION
NAME
SIGNATURE
DATE
DRAWN
CHK'D
APP'D
MFG
Q.A
MATERIAL:
WEIGHT:
TITLE:
Cutting Adjustment System
DWG NO.
Guia_corte
A4
SCALE:2:1
SHEET 1 OF 1

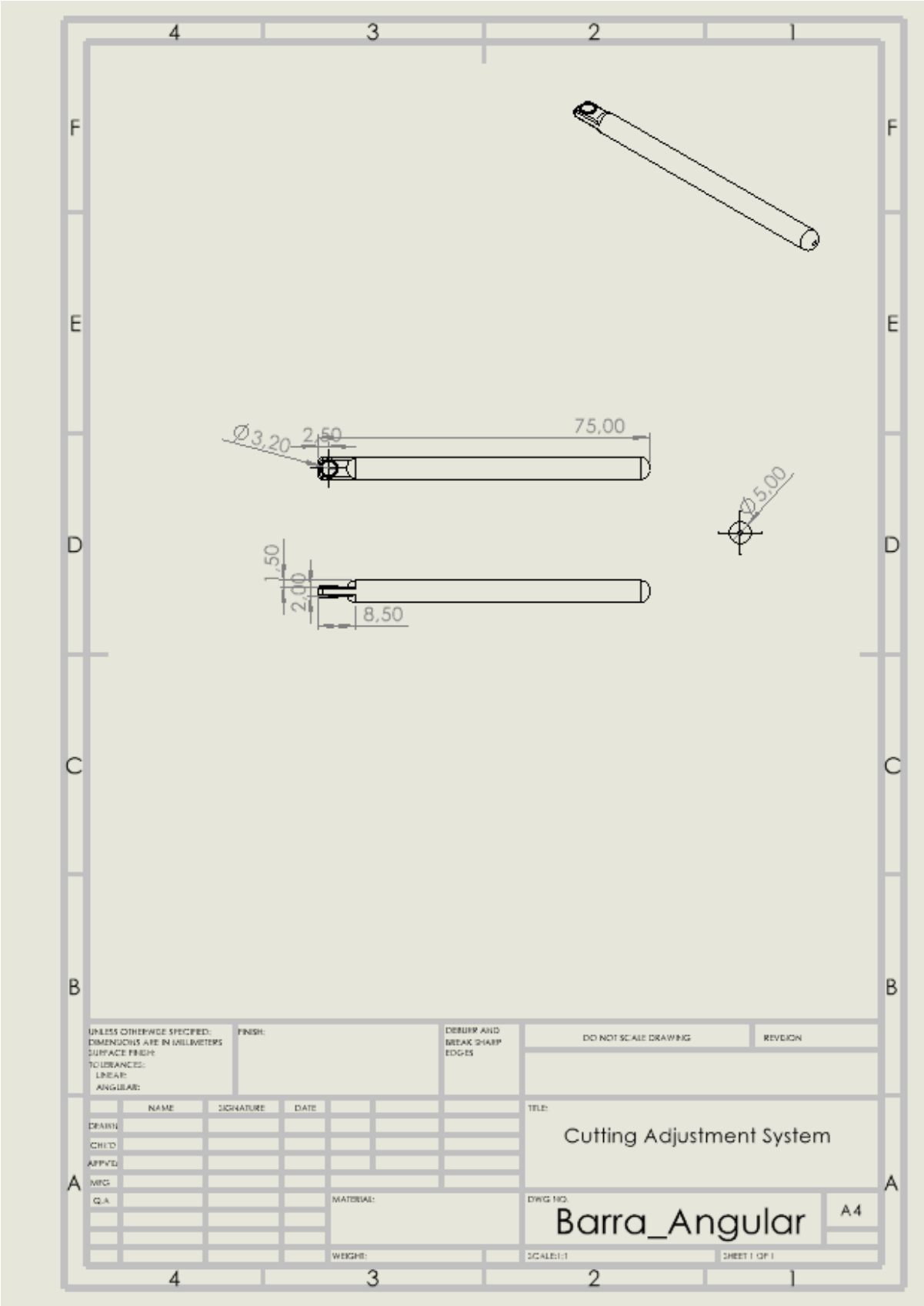
4
3
2
1
F
E
D
C
B
A
Ø3,20
2,50
75,00
Ø5,00
1,50
2,00
8,50
UNLESS OTHERWISE SPECIFIED:
DIMENSIONS ARE IN MILLIMETERS
SURFACE FINISH:
TOLERANCES:
LINEAR:
ANGULAR:
FINISH:
DEBURR AND
BREAK SHARP
EDGES
DO NOT SCALE DRAWING
REVISION
NAME
SIGNATURE
DATE
DRAWN
CHK'D
APPV'D
MFG
Q.A
MATERIAL:
WEIGHT:
TITLE:
Cutting Adjustment System
DWG NO.
Barra_Angular
A4
SCALE:1:1
SHEET 1 OF 1

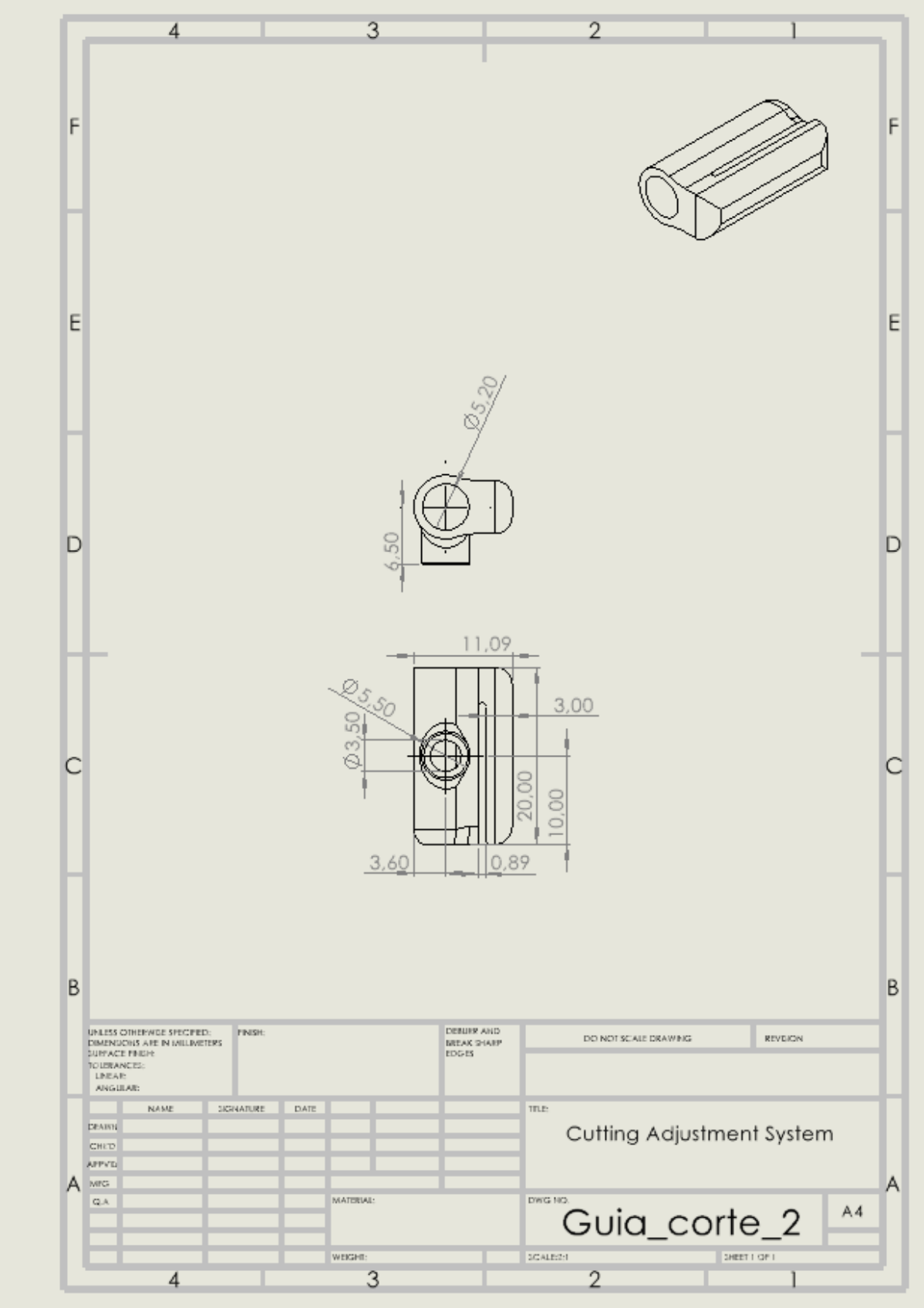
4
3
2
1
F
E
D
C
B
A
Ø5,20
6,50
11,09
Ø5,50
Ø3,50
3,00
20,00
10,00
3,60
0,89
UNLESS OTHERWISE SPECIFIED:
DIMENSIONS ARE IN MILLIMETERS
SURFACE FINISH:
TOLERANCES:
LINEAR:
ANGULAR:
FINISH:
DEBURR AND BREAK SHARP EDGES
DO NOT SCALE DRAWING
REVISION
NAME
SIGNATURE
DATE
DRAWN
CHK'D
APP'D
MFG
Q.A
MATERIAL:
WEIGHT:
TITLE:
Cutting Adjustment System
DWG NO.
Guia_corte_2
A4
SCALE:2:1
SHEET 1 OF 1

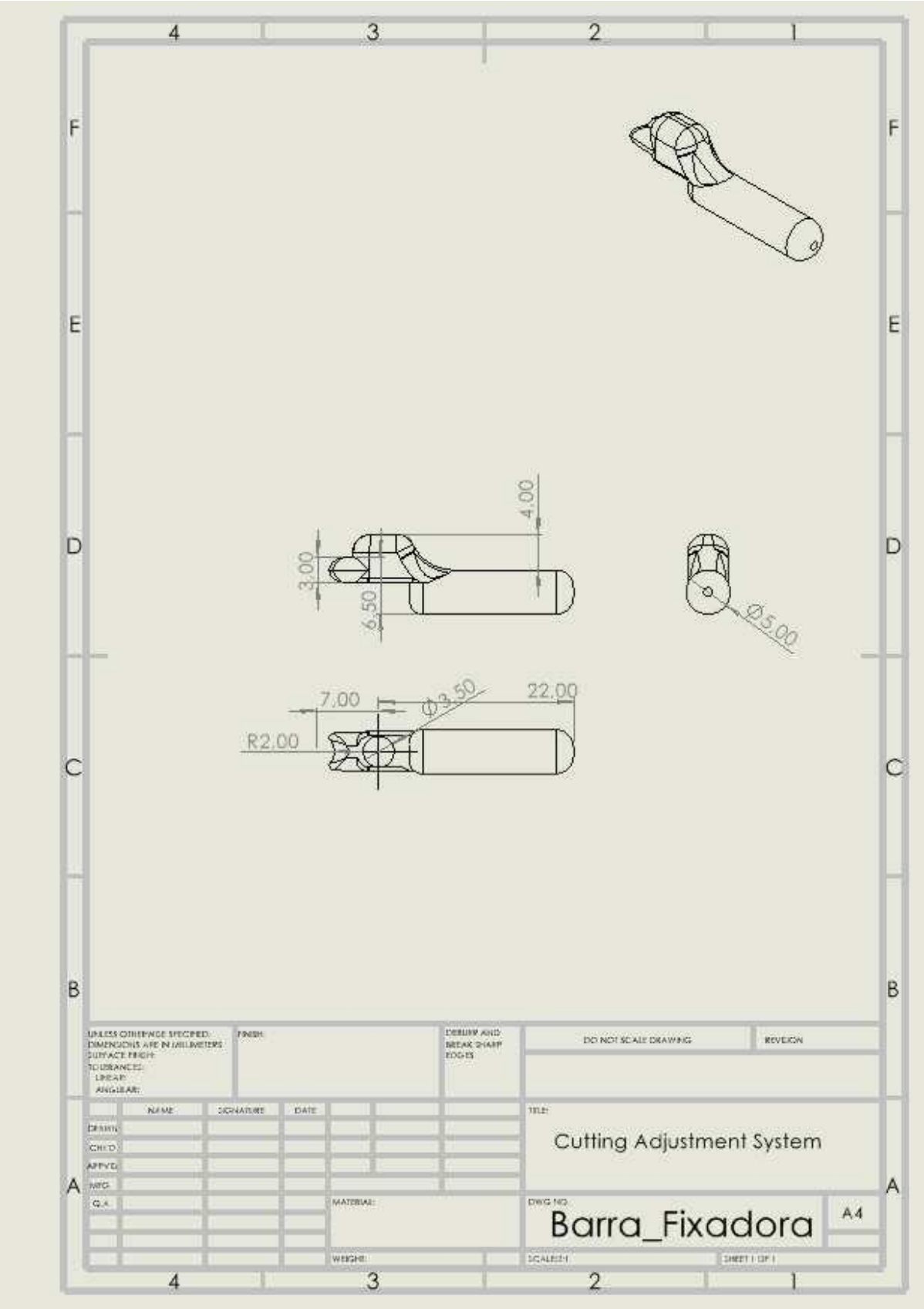
4.00
3.00
6.50
Ø5.00
7.00
Ø3.50
22.00
R2.00
Cutting Adjustment System
Barra_Fixadora
A4

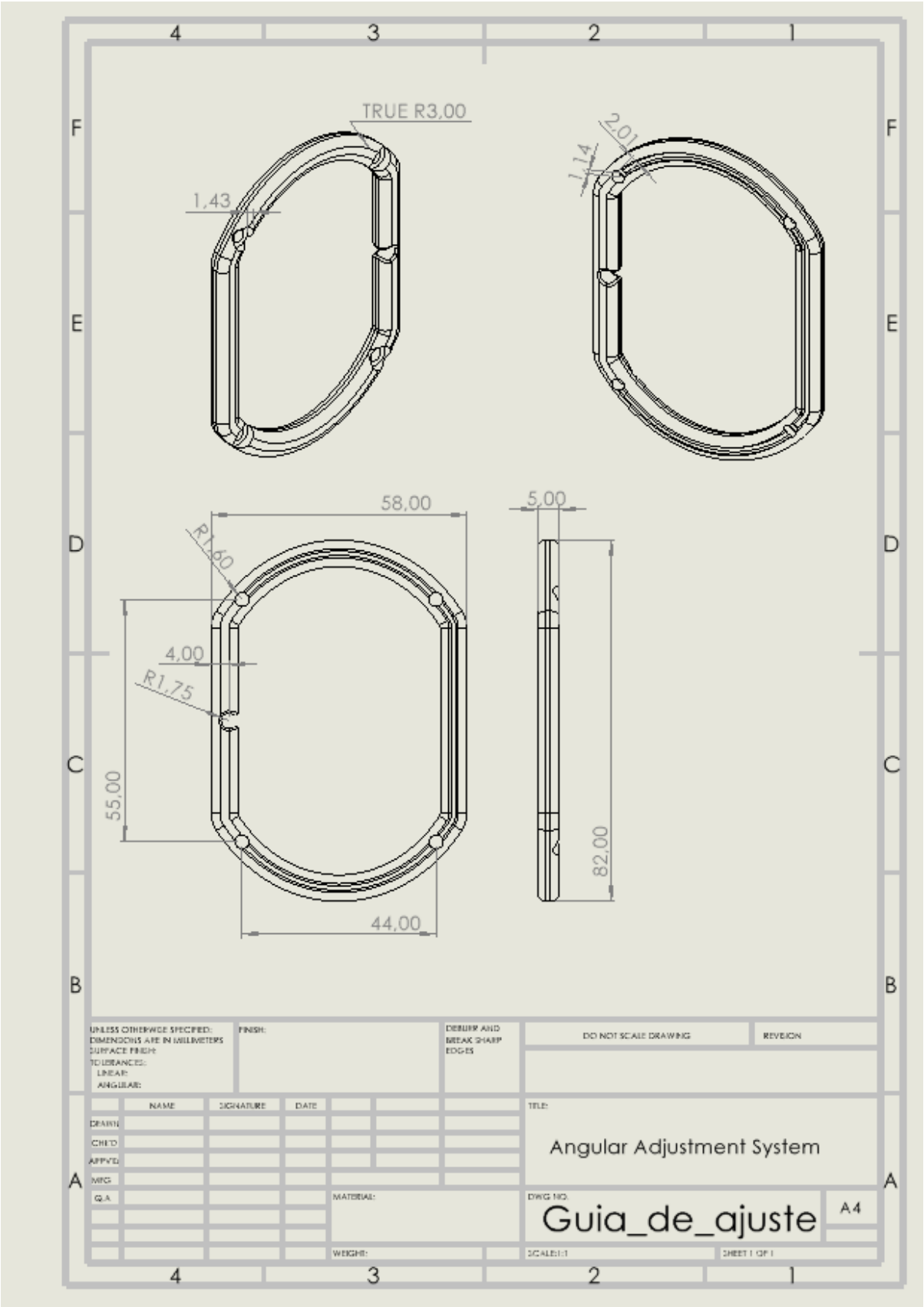
TRUE R3,00
1,43
2,01
1,14
58,00
5,00
R1,60
4,00
R1,75
55,00
82,00
44,00
UNLESS OTHERWISE SPECIFIED:
DIMENSIONS ARE IN MILLIMETERS
SURFACE FINISH:
TOLERANCES:
LINEAR:
ANGULAR:
FINISH:
DEBURR AND BREAK SHARP EDGES
DO NOT SCALE DRAWING
REVISION
NAME
SIGNATURE
DATE
DRAWN
CHK'D
APPV'D
MFG
Q.A
MATERIAL:
WEIGHT:
TITLE:
Angular Adjustment System
DWG NO.
Guia_de_ajuste
A4
SCALE:1:1
SHEET 1 OF 1

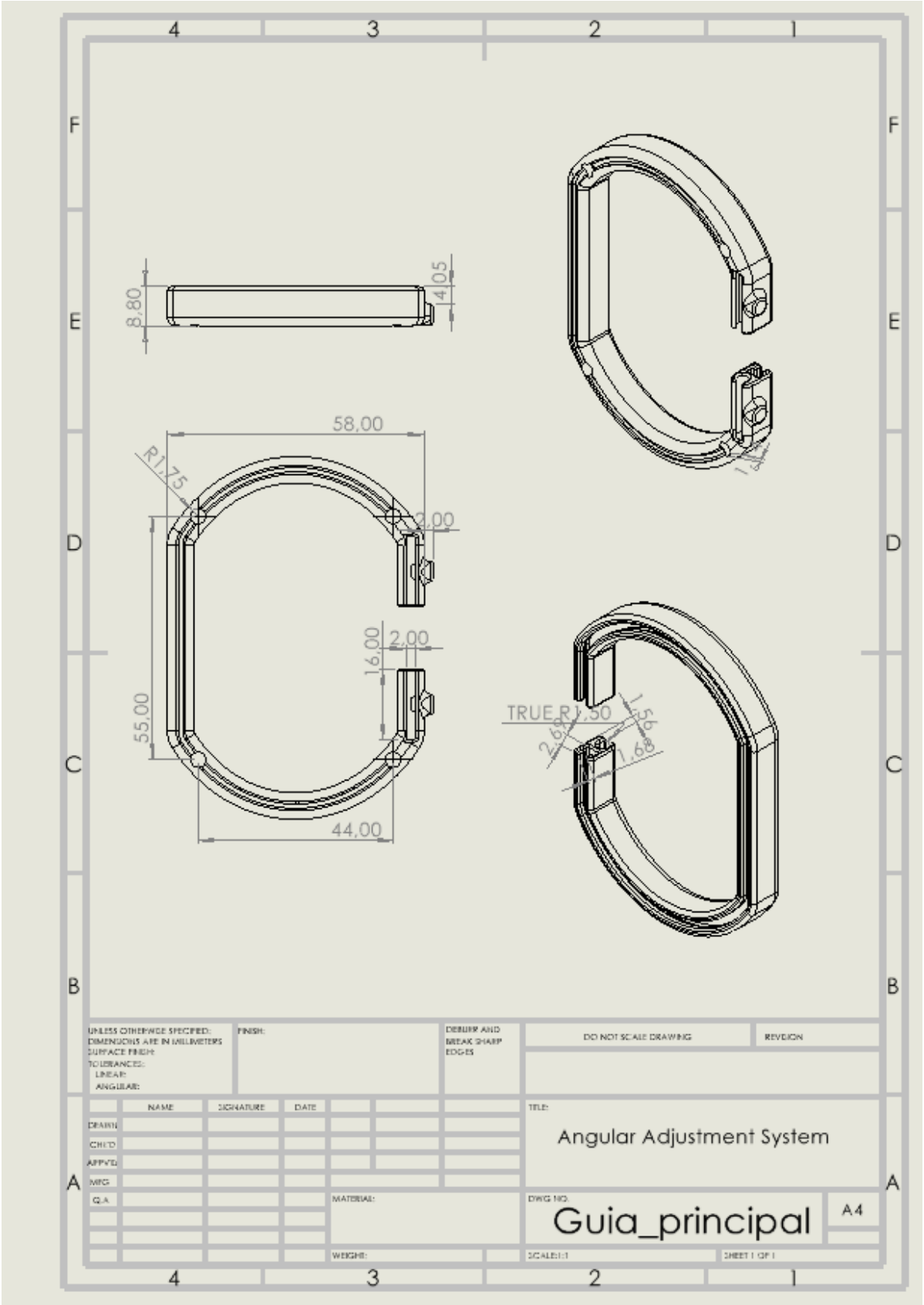
8,80
4,05
58,00
R1,75
2,00
16,00
2,00
55,00
44,00
TRUE R1,50
1,56
2,68
1,68
UNLESS OTHERWISE SPECIFIED:
DIMENSIONS ARE IN MILLIMETERS
SURFACE FINISH:
TOLERANCES:
LINEAR:
ANGULAR:
FINISH:
DEBURR AND BREAK SHARP EDGES
DO NOT SCALE DRAWING
REVISION
NAME
SIGNATURE
DATE
DRAWN
CHK'D
APPV'D
MFG
Q.A
MATERIAL:
WEIGHT:
TITLE:
Angular Adjustment System
DWG NO.
Guia_principal
A4
SCALE:1:1
SHEET 1 OF 1

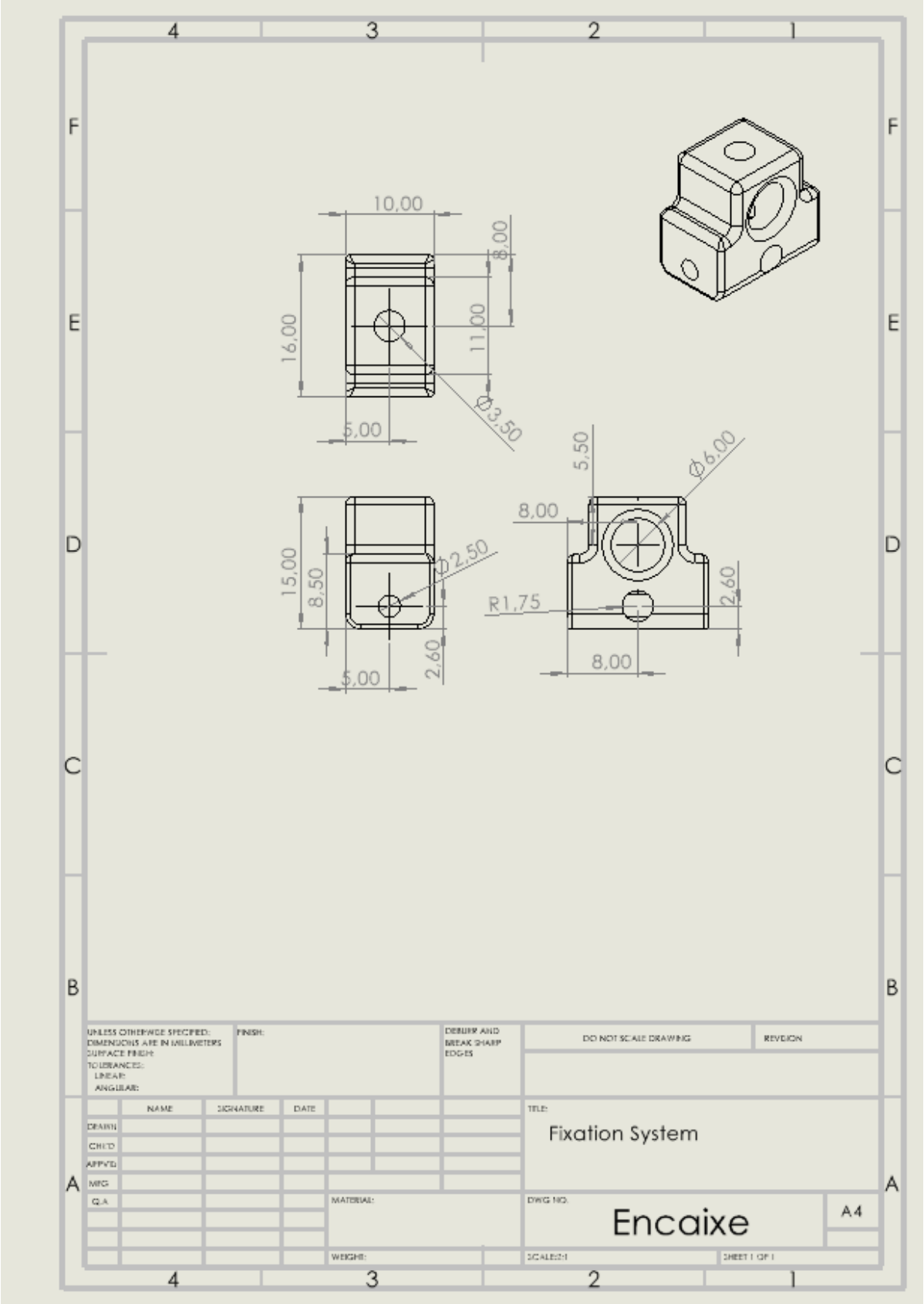
10,00
8,00
16,00
11,00
Ø3,50
5,00
5,50
Ø6,00
8,00
15,00
8,50
Ø2,50
R1,75
2,60
5,00
2,60
8,00
UNLESS OTHERWISE SPECIFIED:
DIMENSIONS ARE IN MILLIMETERS
SURFACE FINISH:
TOLERANCES:
LINEAR:
ANGULAR:
FINISH:
DEBURR AND BREAK SHARP EDGES
DO NOT SCALE DRAWING
REVISION
NAME
SIGNATURE
DATE
DRAWN
CHK'D
APP'D
MFG
Q.A
MATERIAL:
WEIGHT:
TITLE:
Fixation System
DWG NO.
Encaixe
A4
SCALE:1:1
SHEET 1 OF 1

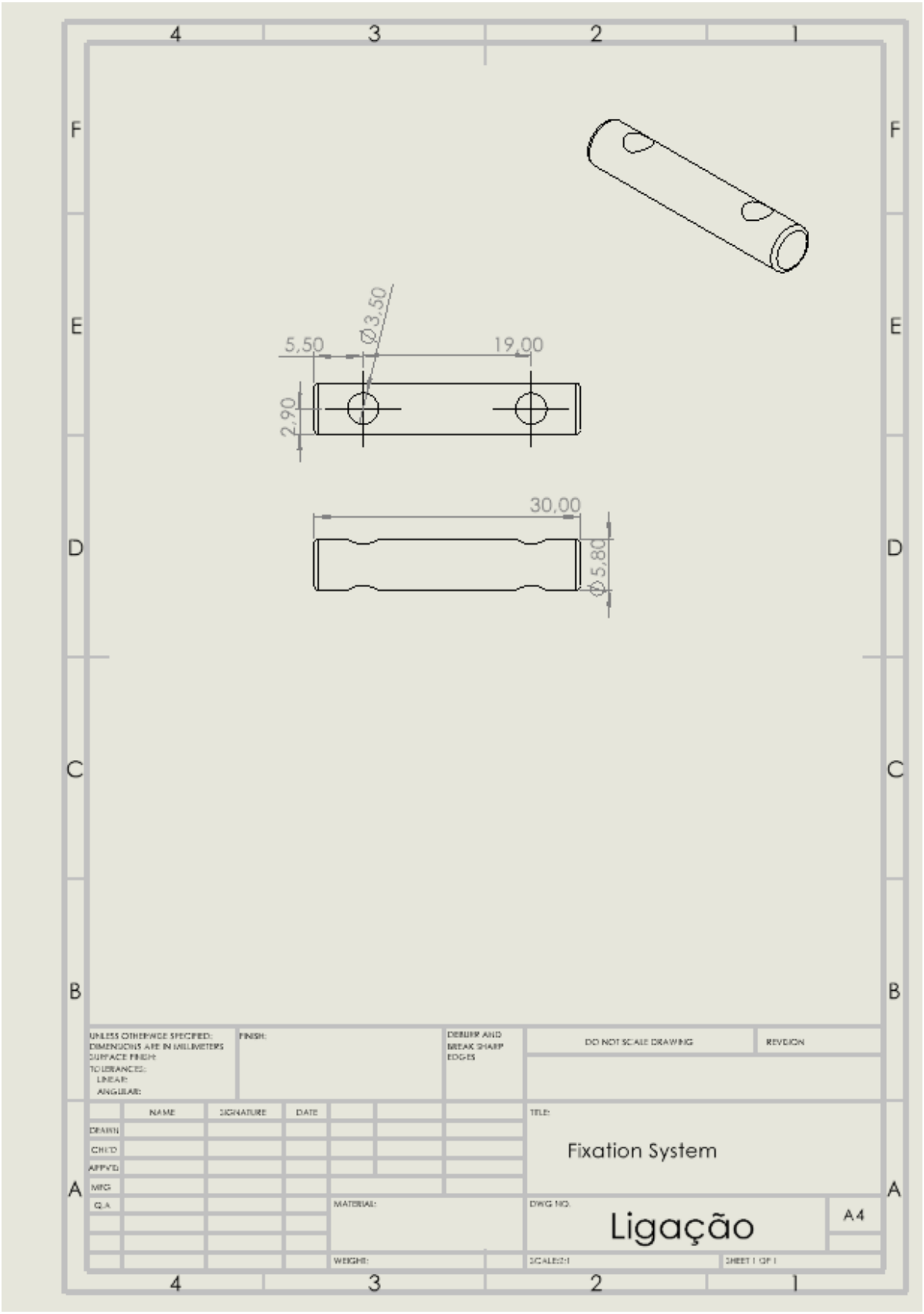
4
3
2
1
F
E
D
C
B
A
5,50
Ø3,50
19,00
2,90
30,00
Ø5,80
UNLESS OTHERWISE SPECIFIED:
DIMENSIONS ARE IN MILLIMETERS
SURFACE FINISH:
TOLERANCES:
LINEAR:
ANGULAR:
FINISH:
DEBURR AND
BREAK SHARP
EDGES
DO NOT SCALE DRAWING
REVISION
NAME
SIGNATURE
DATE
DRAWN
CHK'D
APPV'D
MFG
Q.A
MATERIAL:
WEIGHT:
TITLE:
Fixation System
DWG NO.
Ligação
A4
SCALE:2:1
SHEET 1 OF 1

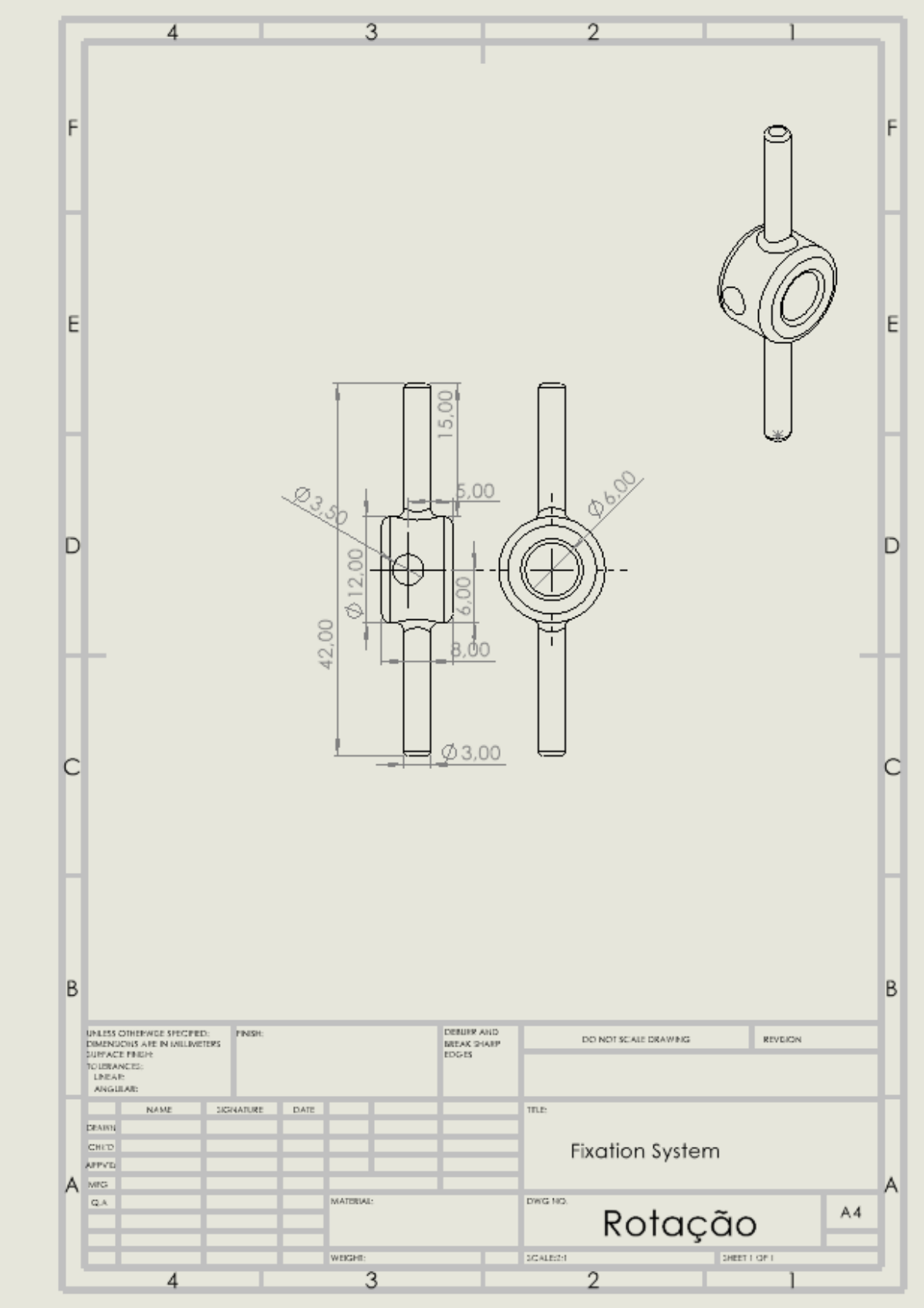
4
3
2
1
F
E
D
C
B
A
15,00
5,00
Ø3,50
Ø12,00
6,00
42,00
8,00
Ø6,00
Ø3,00
UNLESS OTHERWISE SPECIFIED:
DIMENSIONS ARE IN MILLIMETERS
SURFACE FINISH:
TOLERANCES:
LINEAR:
ANGULAR:
FINISH:
DEBURR AND
BREAK SHARP
EDGES
DO NOT SCALE DRAWING
REVISION
NAME
SIGNATURE
DATE
DRAWN
CHKD
APPVD
MFG
Q.A
MATERIAL:
WEIGHT:
TITLE:
Fixation System
DWG NO.
Rotação
A4
SCALE:1:1
SHEET 1 OF 1

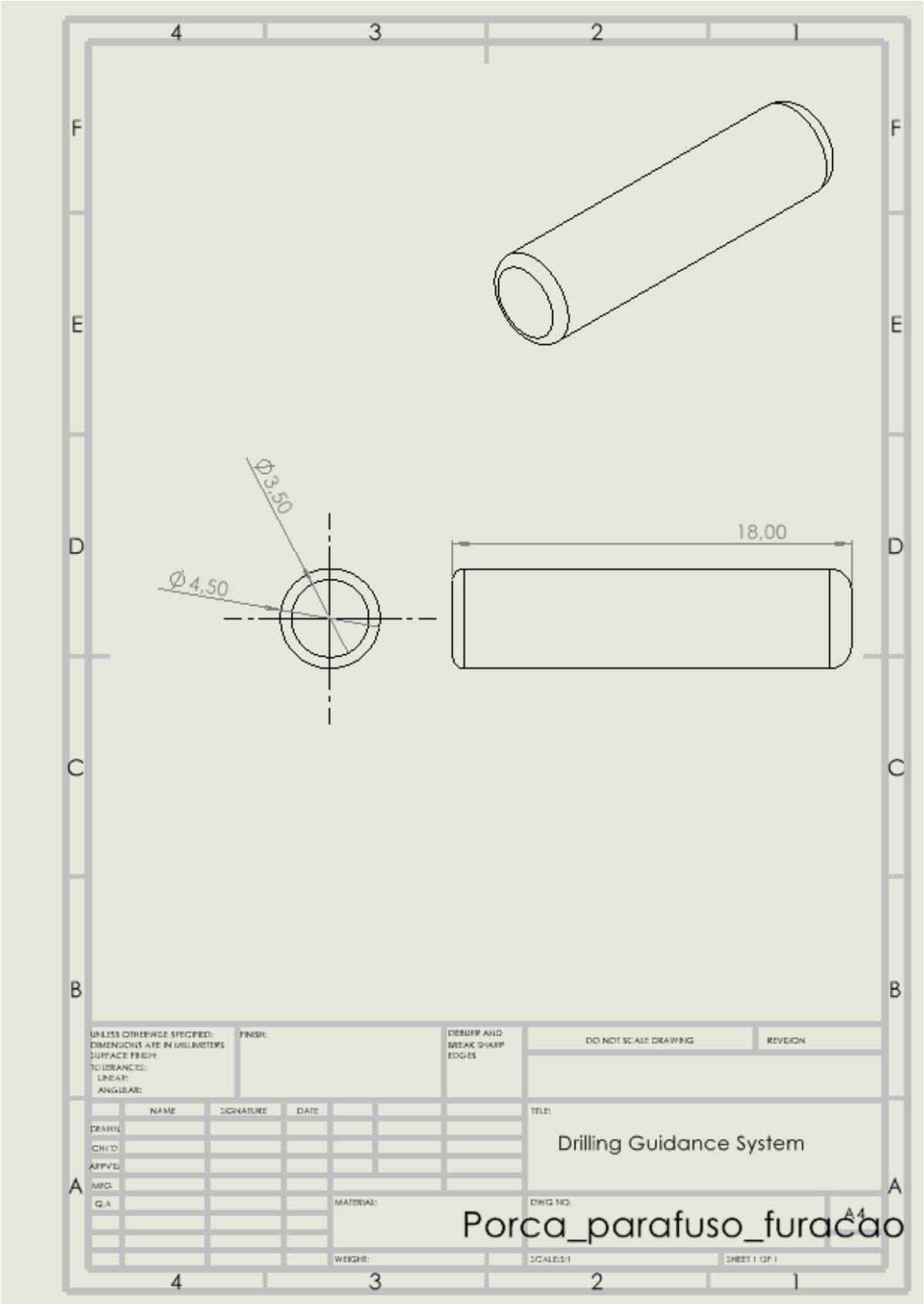
4
3
2
1
F
E
D
C
B
A
Ø3,50
Ø4,50
18,00
UNLESS OTHERWISE SPECIFIED:
DIMENSIONS ARE IN MILLIMETERS
SURFACE FINISH:
TOLERANCES:
LINEAR:
ANGULAR:
FINISH:
DEBURR AND BREAK SHARP EDGES
DO NOT SCALE DRAWING
REVISION
NAME
SIGNATURE
DATE
DRAWN
CHK'D
APPV'D
MFG
Q.A
TITLE:
Drilling Guidance System
MATERIAL:
DWG NO.
A4
Porca_parafuso_furacao
WEIGHT:
SCALE:5:1
SHEET 1 OF 1

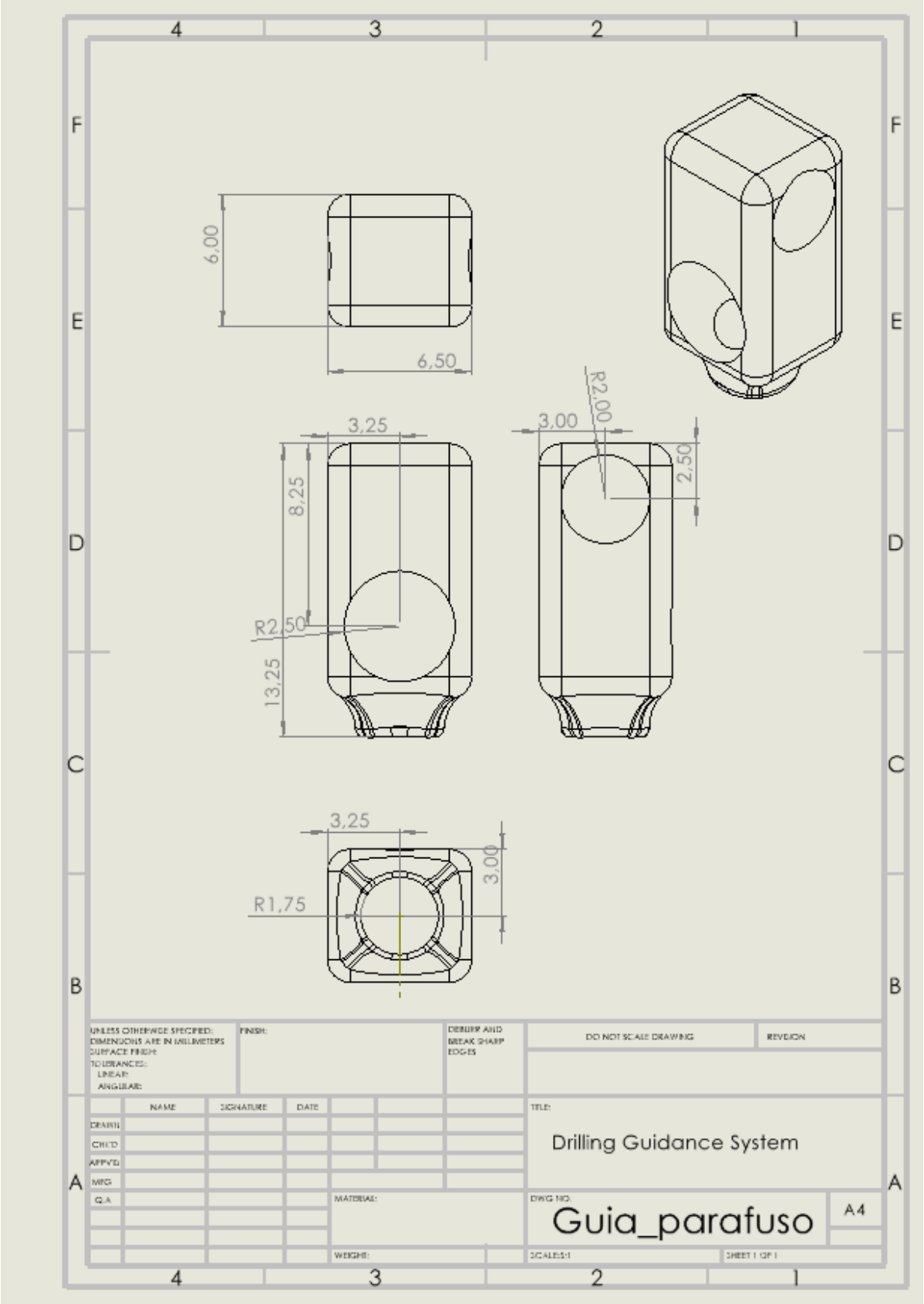
6,00
6,50
3,25
8,25
R2,50
13,25
3,00
R2,00
2,50
3,25
3,00
R1,75
UNLESS OTHERWISE SPECIFIED:
DIMENSIONS ARE IN MILLIMETERS
SURFACE FINISH:
TOLERANCES:
LINEAR:
ANGULAR:
FINISH:
DEBURR AND BREAK SHARP EDGES
DO NOT SCALE DRAWING
REVISION
NAME
SIGNATURE
DATE
DRAWN
CHK'D
APP'D
MFG
Q.A
TITLE:
Drilling Guidance System
MATERIAL:
DWG NO.
Guia_parafuso
A4
WEIGHT:
SCALE:1:1
SHEET 1 OF 1

Appendix B - Bone Model with Multimaterials

New Artificial Bone Model with Multimaterials Additive Manufacturing, the first models in production, obtained can be observed in this appendix.

The images show the first models in production based on multimaterials additive manufacturing.

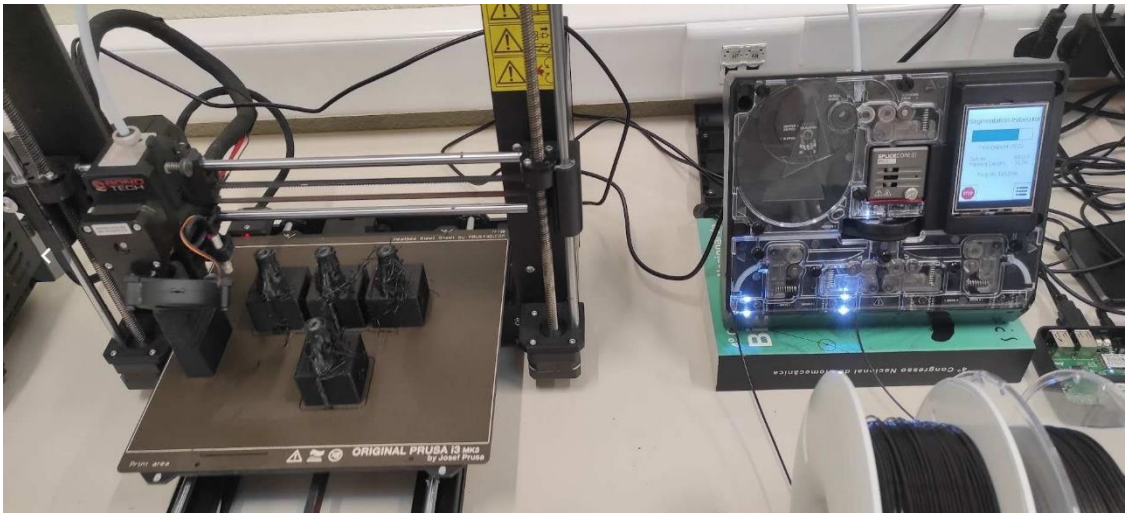

Appendix C - Geometry for Subtractive Production

Device Geometry for Subtractive Production with Aluminum.

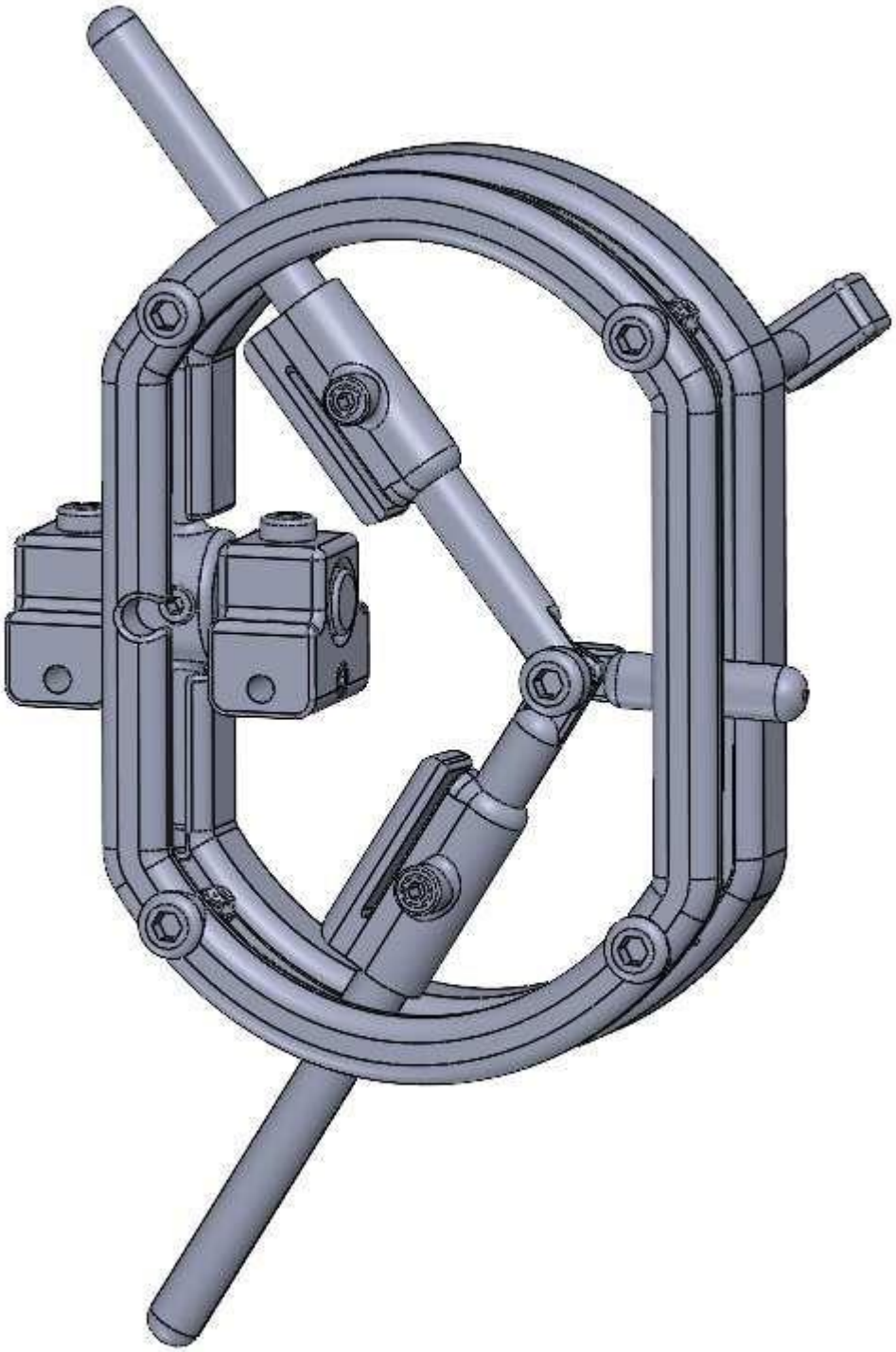

Instituto Superior de Engenharia
Politécnico de Coimbra